1992

Thermally induced stresses in a composite exposed to fire

Faxlanger, Edward Allan, Jr.

Monterey, California. Naval Postgraduate School

REPORT DOCUMENTATION PAGE

1a. REPORT SECURITY CLASSIFICATION Unclassified	1b RESTRICTIVE MARKINGS
2a. SECURITY CLASSIFICATION AUTHORITY	3 DISTRIBUTION/AVAILABILITY OF REPORT Approved for public release; distribution is unlimited.
2b DECLASSIFICATION/DOWNGRADING SCHEDULE	
4 PERFORMING ORGANIZATION REPORT NUMBER(S)	5 MONITORING ORGANIZATION REPORT NUMBER(S)
6a NAME OF PERFORMING ORGANIZATION Naval Postgraduate School 6b OFFICE SYMBOL *(If applicable)* ME	7a NAME OF MONITORING ORGANIZATION Naval Postgraduate School
6c. ADDRESS (*City, State, and ZIP Code*) Monterey, CA 93943-5000	7b ADDRESS (*City, State, and ZIP Code*) Monterey, CA 93943-5000
8a NAME OF FUNDING/SPONSORING ORGANIZATION 8b OFFICE SYMBOL *(If applicable)*	9 PROCUREMENT INSTRUMENT IDENTIFICATION NUMBER
8c. ADDRESS (*City, State, and ZIP Code*)	10 SOURCE OF FUNDING NUMBERS Program Element No / Project No / Task No / Work Unit Accession Number

11. TITLE (*Include Security Classification*)
THERMALLY INDUCED STRESSES IN A COMPOSITE EXPOSED TO FIRE

12. PERSONAL AUTHOR(S) EDWARD ALLAN FAXLANGER JR.

13a TYPE OF REPORT	13b TIME COVERED	14 DATE OF REPORT (*year, month, day*)	15 PAGE COUNT
Master's Thesis	From To	December 1992	98

16. SUPPLEMENTARY NOTATION
The views expressed in this thesis are those of the author and do not reflect the official policy or position of the Department of Defense or the U.S. Government.

17 COSATI CODES			18 SUBJECT TERMS (*continue on reverse if necessary and identify by block number*)
FIELD	GROUP	SUBGROUP	fire, composite, epoxy, graphite, stresses,

19. ABSTRACT (*continue on reverse if necessary and identify by block number*)

This thesis investigates the behavior of graphite/epoxy composites subjected to fire as may occur on the decks of naval aircraft carriers. The analytical model cosists of two parts: one for the determination of the temperature field within the composite due to a fire, and the other for determining the stresses within the composite due to the temperature field. Both problems are provided one-dimensional finite element models. Appropriate failure criteria are incorporated to predict the survivability of composites in various fire environments. Parametric studies were performed and the results are presented in both graphical and tabular form.

20 DISTRIBUTION/AVAILABILITY OF ABSTRACT	21 ABSTRACT SECURITY CLASSIFICATION	
☒ UNCLASSIFIED/UNLIMITED ☐ SAME AS REPORT ☐ DTIC USERS	Unclassified	
22a NAME OF RESPONSIBLE INDIVIDUAL David Salinas	22b TELEPHONE (*Include Area code*) 408-646-3426	22c. OFFICE SYMBOL ME/SA

DD FORM 1473, 84 MAR 83 APR edition may be used until exhausted
All other editions are obsolete

SECURITY CLASSIFICATION OF THIS PAGE

UNCLASSIFIED

Approved for public release; distribution is unlimited.

Thermally Induced Stresses in a Composite Exposed to Fire

by

Edward Allan Faxlanger Jr.
Lieutenant, United States Navy
B.S.Ch.E.,University of South Carolina, 1987

Submitted in partial fulfillment
of the requirements for the degree of

MASTER OF SCIENCE IN MECHANICAL ENGINEERING

from the

NAVAL POSTGRADUATE SCHOOL
DECEMBER 1992

ABSTRACT

This thesis investigates the behavior of Graphite-Epoxy composites subjected to fires as may occur on the decks of naval aircraft carriers. The analytical model consists of two parts; one for the determination of the temperature field within the composite due to a fire and the other for determining the stresses within the composite due to the temperature field. Both problems are provided one-dimensional finite element models. Appropriate failure criteria are incorporated to predict the survivability of composites in various fire environments. Parametric studies were performed with the results presented in both graphical and tabular form.

TABLE OF CONTENTS

LIST OF FIGURES

I. INTRODUCTION

A. BACKGROUND

Composite materials, due to their high strength to weight ratio, are becoming increasingly common as construction materials in today's modern combat aircraft. Through use of these materials the weight to strength ratio of the airframe has been greatly reduced allowing for an increase in the respective payload per unit weight of the structure.

Several different Navy fixed wing aircraft such as the F-18, F-16, F-15 and F-14 all use composite materials in their construction. Since these aircraft are used on board naval aircraft carriers, it is quite conceivable that these structures could be exposed to flight deck fires of varying intensities during their service life. It is important for the Navy to assess the survivability of composite aircraft exposed to fires. To this end, experimental and analytical investigations have been undertaken.

In 1979 testing was performed at the Naval Weapons Center (China Lake) to determine the relative survivability of Graphite-Epoxy Composite materials and 7075-T6 Aluminum Alloy when exposed to flight deck pool fires [Ref. 1]. These tests indicated the susceptibility to burn through for Graphite-Epoxy samples was approximately the same as for the comparable

7075-T6 Aluminum Alloy samples tested. However unlike the aluminum, in some cases the composite material continued to smolder and/or burn after application of extinguishing agents. In an attempt to model this smoldering/burning of Graphite-Epoxy Composites, Vatikiotis in 1980 [Ref. 2] developed a computer model which he later refined in 1982 [Ref. 3]. This finite element program evaluates fiber diameters, fiber temperatures, air temperatures and oxygen levels throughout Graphite-Epoxy materials exposed to fire. The evaluations are with respect to time and location.

Graphite-Epoxy material consists of high strength graphite fibers surrounded by an epoxy matrix. When exposed to a fire the epoxy matrix material burns off rather quickly at 400-500^{o}F leaving only the graphite fibers supported by residual combustion products. These remaining high strength fibers develop thermally induced stresses due to the varying temperature profile across the material. If high enough stresses are developed, fibers may fail rendering the remaining material of no structural use. However, if a considerable amount of fibers do not fail the surviving material, although considerably weakened in the compression mode, could continue to be used in the tensile mode.

B. OBJECTIVE OF THIS THESIS

This thesis investigated thermally induced stress failure of Graphite-Epoxy material exposed to varying intensity fires.

The analysis was carried out in two parts. In part one, the computer model developed by Vatikiotis in 1982 was used to model fires of different intensities. This program evaluated the temperature profiles across a porous medium consisting of graphite fibers as time progressed. These results were further utilized in the second part of the analysis. Part two of the analysis consisted of developing a stress model and finite element computer program. This stress code evaluated the thermally induced stresses of fibers based on the temperature profiles determined from the combustion code. The fiber stresses were calculated at each time step; failure criteria applied and failed fibers removed from the stress analysis. Through this procedure, a quantitative evaluation of Graphite-Epoxy material failure with respect to time was obtained.

C. THESIS OUTLINE

Chapter II presents the physical and mathematical models.

Chapter III develops the failure criteria used in determination of individual fiber failure.

Chapter IV contains a description of the stress analysis program and it's interaction with the combustion program developed by Vatikiotis.

Chapter V presents case studies with results presented in graphical form.

Chapter VI contains the conclusions.

II. PROBLEM FORMULATION

A. PHYSICAL MODEL

The physical model assumed for this study is that of a Graphite-Epoxy composite plate exposed to fires of varying intensity as shown in Figure 1. This plate of composite material could have several different nominal thicknesses depending on the number of laminate layers or ply assumed. For this study, nominal thicknesses of 0.25, 0.5, 0.75 and 1.0 inch are assumed, corresponding to approximately 35, 70, 105 and 140 ply composites respectively.

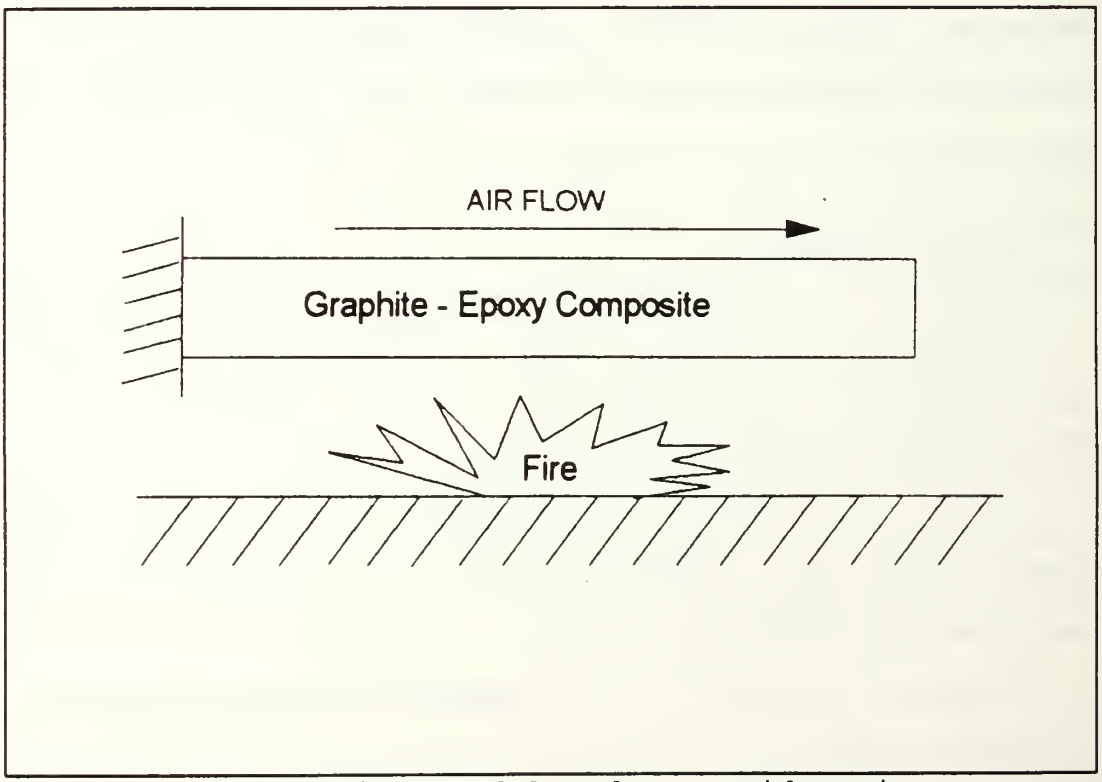

Figure 1: The physical model under consideration.

As the composite plate heats up it will lose its epoxy matrix material between 400 and 500°F. The matrix loss process is too complex to model exactly. However, for epoxy loss to occur, the epoxy matrix must undergo phase changes from solid to combustion products. These phase changes occur at a constant temperature throughout the material.

This study assumes that no failure of graphite fibers occurs prior to the burn-off of the epoxy matrix material. The point at which the epoxy matrix has been reduced to residue will be chosen as the starting time for all case studies. Because of the phase changes which occur during the matrix burn off process described above, the initial temperature profile across the remaining Graphite fiber medium is assumed to be a constant 400°F at the starting time.

Air flows across the upper surface of the composite plate. This surface air flow produces a differential pressure across the thickness of the plate. At the starting time for these studies, since the matrix material has been removed, this differential pressure will induce air flow perpendicular through the remaining composite plate.

B. VATIKIOTIS COMBUSTION MODEL

In order to obtain the temperature field required for stress analysis the one-dimensional finite element program developed by Vatikiotis was used. As seen in Figure 2 his combustion model assumes the composite material has been

exposed to heat sufficient to remove the epoxy matrix leaving only the graphite fibers surrounded by air filled voids. The heat supplied by the fire is implemented through application of a constant heat flux boundary condition at the lower, X=0, surface. Differential pressure across the plate thickness forces air flow through the material. Prior to fiber combustion the incoming air is considered to be of standard composition containing no fire combustion products. After combustion begins carbon dioxide and carbon monoxide also flow through the material.

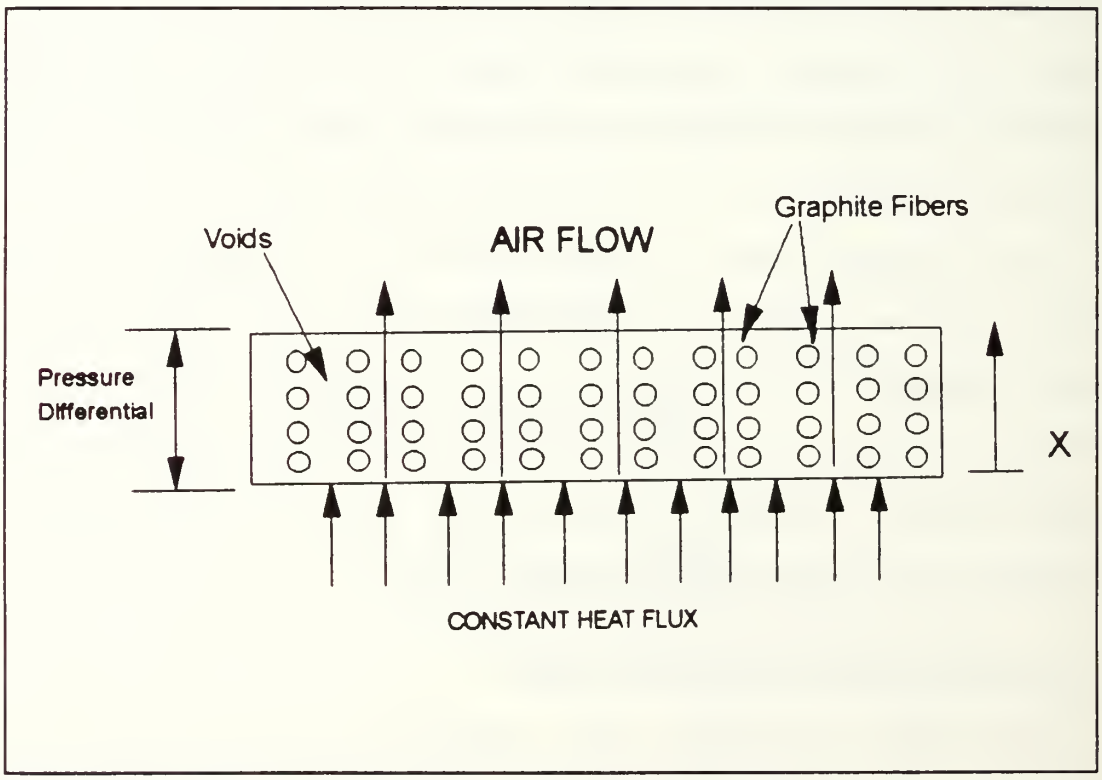

Figure 2: The Vatikiotis combustion model.

In his presentation Vatikiotis divides the material across its thickness into 30 equal thickness elements having a total

of 31 nodal points. He further develops a system of four transient one-dimensional equations consisting of an energy balance on the graphite material, an energy balance on the internal air, conservation of species on oxygen and a combination of Darcy's law and continuity equation for internal air flow velocities.

The two energy balances considered a differential volume of material with the following convention:

$$\underset{dV}{\textit{Heat into}} + \underset{\textit{Generation}}{\textit{Heat}} = \underset{dV}{\textit{Heat out of}} + \underset{\textit{Internal Energy}}{\textit{Increased}}$$

The energy balance for the graphite fibers accounted for heat transfer into and out of the differential volume by three modes; conduction, convection and radiation, using first term Taylor series approximations. The heat generation term, resulting from burning of the graphite fibers, was modeled using an expression of Arrhenius type.

The energy balance for the internal air considers only conduction and convection at the differential volume surfaces along with energy transport due to the flow of air through the volume. Also this equation does not contain a heat generation term.

The oxygen mass balance started from the basic form of:

$$\underset{dV}{\textit{Oxygen into}} = \underset{dV}{\textit{Oxygen out of}} + \underset{\textit{Consumption}}{\textit{Oxygen}} + \underset{\textit{Accumulation}}{\textit{Oxygen}}$$

The oxygen into and out of the differential volume considers both molecular diffusion and convective transport

across the differential volume surfaces, again using a first term Taylor series approximations. The oxygen consumption was based on the graphite fibers (carbon) burning with the oxygen present, in a appropriately specified stoichiometric ratio. This reaction is assumed to produce carbon dioxide and carbon monoxide only. A relationship for the consumption of oxygen was developed through combination of the stoichiometric ratio with the Arrhenius reaction rate equation.

The final equation of this system is the equation for internal air flow velocities. This equation was developed using a combination of Darcy's law for flow in a porus medium and the continuity equation.

The above four equations form a set of coupled, nonlinear, transient, partial differential equations. These equations are solved for graphite temperature, air temperature, oxygen concentration, and internal air flow velocities with respect to time and position. Incorporated in this mathematical model are the variations of temperature dependent properties namely, graphite thermal conductivity, fluid (air) viscosity, and air density, along with parameters derived from them. These properties and parameters are recalculated at each time step of the transient solution. The Darcy's law-continuity equation was solved using a shooting method and the remaining three equations were solved using a Galerkin formulation of the finite element method. For completeness the above equations in their final form along with their associated

boundary conditions are contained in Appendix A. For more in depth review the reader is referred to Vatikiotis' original works.

The main observations of Vatikiotis' earlier work are very obvious when his computer code is used. The differential pressure across the porous medium causes a flow of air to flow through medium. This induced air flow provides for both convective heat transfer of the fibers and a ready supply of oxygen for the combustion process. These two effects of the air flow are conflicting effects. First, the supply of oxygen increases the rate of combustion which increases the fiber temperature. Second, the convective heat transfer away from the hot fibers reduces the fiber temperature. A system comprised of a plate and a fire is defined by (a) the fire intensity and its time duration and (b) the plate subjected to the fire. A plate with known initial temperatures and oxygen concentrations, thickness, porosity, and pressure differential is subjected to a fire of specified intensity for a given time period. When the fire is removed the plate may either continue to burn (plate combustion) or the plate may return to ambient conditions (plate extinction). Which process occurs depends on the state of the plate when the fire has been removed. If the temperature and air velocity fields exceed a critical state then the convective heat transfer from the fibers to the air is overtaken by the heat generated by the fiber combustion and the material will continue to burn. If

the critical state was not achieved, the convective heat transfer will predominate resulting in cooling and extinction.

C. STRESS ANALYSIS MODEL

The combustion model described previously determines the temperature distribution across the thickness of the medium. The stress analysis model uses the temperature profiles from the combustion code to determine the thermally induced stresses in the fiber composite plate.

As seen in Figure 3 the stress model was developed assuming the graphite fibers were cylindrical rods running parallel to the plate surfaces. These fiber rods are modeled as rigidly fixed at one end and on the opposite end are modeled to move in unison with the other fibers. The expansion or contraction of fibers due to varying temperatures will cause forces to develop in the other fibers (See Figure 4). These resulting forces could cause excessive stresses to develop possibly causing failure. The final solution to this statically indeterminate problem required use of finite element techniques.

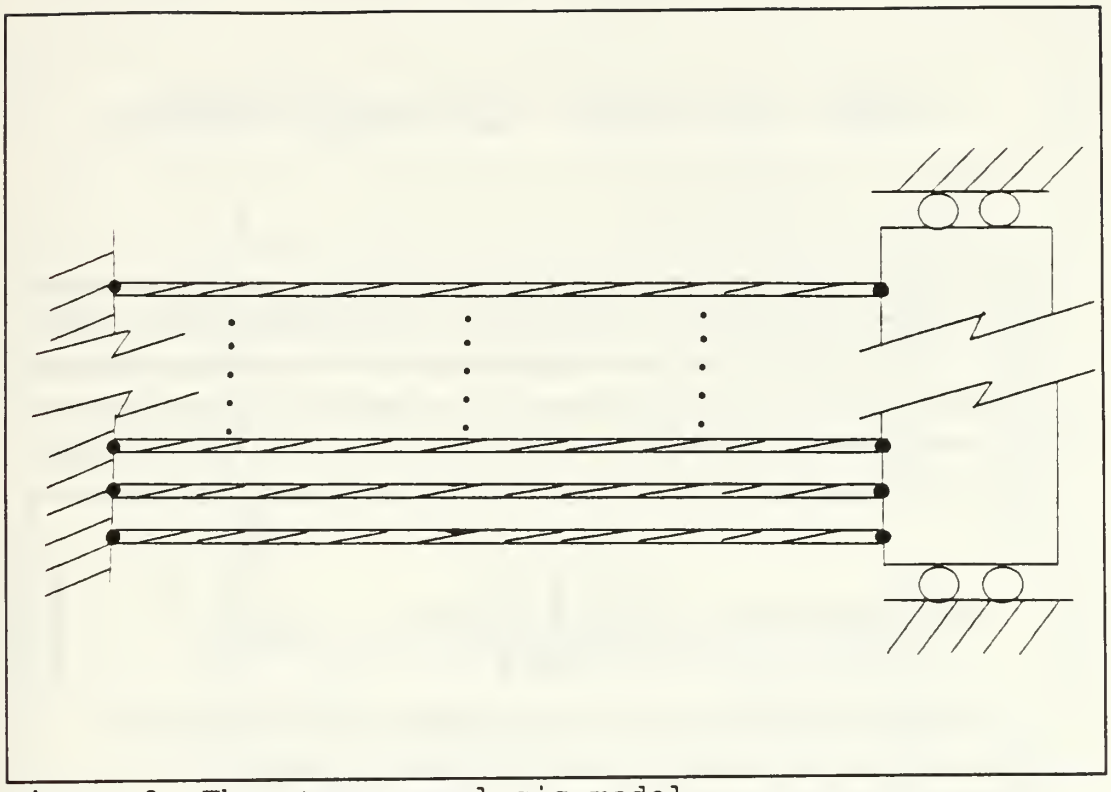

Figure 3: The stress analysis model.

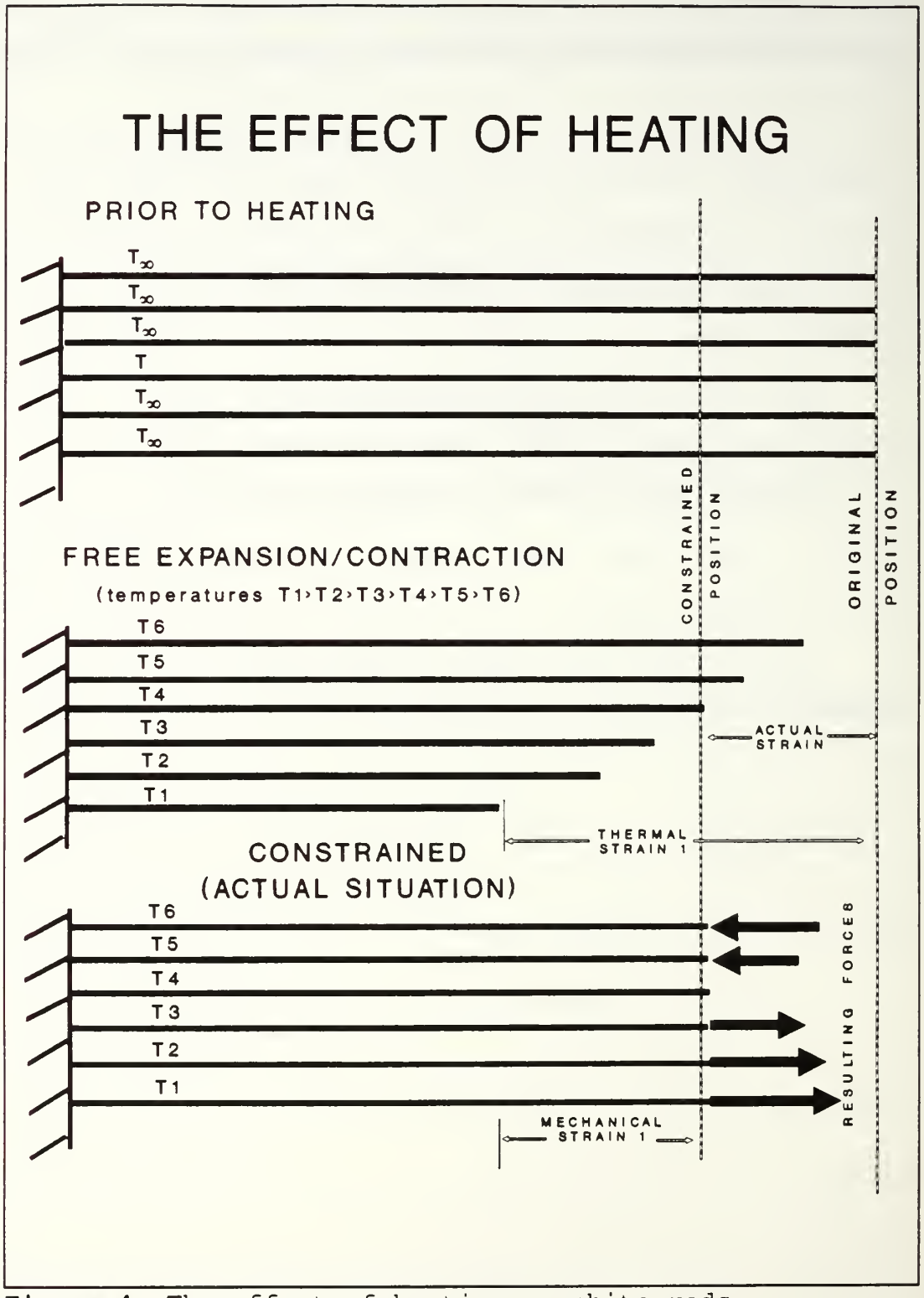

Figure 4: The effect of heating graphite rods.

As seen in Figure 5 each element (fibers per ply) was modeled as a linear elastic spring with forces applied at each end (nodal point). The finite element "direct approach" [Ref. 7] was applied to each individual element to obtain the element stiffness matrix and force vector as follows. All forces, displacements, stresses, strains and element characteristics are in the axial direction only.

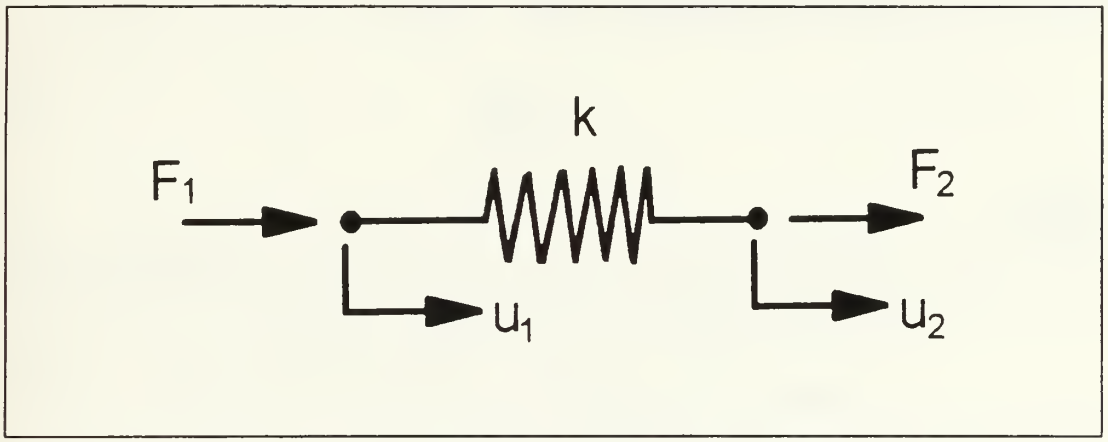

Figure 5: The linear spring element of the finite element direct approach.

First referring to Figure 5, using summation of forces:

$$\sum F = F_1 + F_2 = 0 \tag{2.1}$$

$$F_1 = -F_2 \tag{2.1a}$$

where:

F_1 = force applied at point 1

F_2 = force applied at point 2

Assuming a linear spring model yields:

$$F_2 = k(u_2 - u_1) \tag{2.2}$$

where:

u_1 = displacement of point 1

u_2 = displacement of point 2

k = stiffness coefficient.

From [Ref. 4] the stiffness coefficient for a cylindrical rod with axial displacement is:

$$k = \frac{AE}{L} \tag{2.3}$$

where:

A = cross sectional area of the bar (fibers per ply)

E = elastic modulus of fiber (axial)

L = length of fiber.

Combining equations (2.1a) and (2.2) yields the element matrix equations of:

$$\begin{bmatrix} k & -k \\ -k & k \end{bmatrix}_n \begin{Bmatrix} u_1 \\ u_2 \end{Bmatrix}_n = \begin{Bmatrix} F_1 \\ F_2 \end{Bmatrix}_n \tag{2.4}$$

for fibers, where n is the ply number. The forces F_1 and F_2 are equal in magnitude and come from the thermal expansion of the material as follows.

The thermal strain of the material is defined as:

$$\epsilon_{th} = \alpha (T - T_\infty) \tag{2.5}$$

where:

ϵ_{th} = thermal strain

α = thermal coefficient of expansion

T = the temperature of the material

T_∞ = the temperature at which the strain is zero.

Multiplication of equation (2.5) by Youngs modulus E yields the stress σ,

$$\sigma = E\epsilon = E\alpha (T - T_\infty) \tag{2.6}$$

which results if free expansion or contraction is prevented. Multiplying equation (2.6) by the cross sectional area of the element yields the element forces:

$$- F_{1_n} = F_{2_n} = \sigma A = AE\alpha (T_n - T_\infty) \tag{2.7}$$

at the ends of the elements where n is the ply number. Dropping the subscripts 1 and 2 on the forces and combining equation (2.7) with (2.4) and (2.3) gives the following matrix equations for each element:

$$\begin{bmatrix} k & -k \\ -k & k \end{bmatrix}_n \begin{Bmatrix} u_1 \\ u_2 \end{Bmatrix}_n = \begin{Bmatrix} F \\ F \end{Bmatrix}_n \tag{2.8}$$

where:

k = AE/L based on fiber properties and dimensions

u_1 & u_2 = displacements of points 1 & 2 for fiber n

F = $AE\alpha(T-T_\infty)$.

Using the numbering system of Figure 6, the global stiffness matrix and global force vector are assembled as:

(2.9)

$$\begin{bmatrix} k_1 & -k_1 & 0 & 0 & 0 & 0 & 0 & 0 & 0 & 0 & \cdot & \cdot \\ -k_1 & k_1 & 0 & 0 & 0 & 0 & 0 & 0 & 0 & 0 & \cdot & \cdot \\ 0 & 0 & k_2 & -k_2 & 0 & 0 & 0 & 0 & 0 & 0 & \cdot & \cdot \\ 0 & 0 & -k_2 & k_2 & 0 & 0 & 0 & 0 & 0 & 0 & \cdot & \cdot \\ 0 & 0 & 0 & 0 & k_3 & -k_3 & 0 & 0 & 0 & 0 & \cdot & \cdot \\ 0 & 0 & 0 & 0 & -k_3 & k_3 & 0 & 0 & 0 & 0 & \cdot & \cdot \\ 0 & 0 & 0 & 0 & 0 & 0 & k_4 & -k_4 & 0 & 0 & \cdot & \cdot \\ 0 & 0 & 0 & 0 & 0 & 0 & -k_4 & k_4 & 0 & 0 & \cdot & \cdot \\ \cdot & \cdot & \cdot & \cdot & \cdot & \cdot & \cdot & \cdot & \cdot & \cdot & \cdot & \cdot \\ \cdot & \cdot & \cdot & \cdot & \cdot & \cdot & \cdot & \cdot & \cdot & \cdot & \cdot & \cdot \end{bmatrix} \begin{Bmatrix} U_1 \\ U_2 \\ U_3 \\ U_4 \\ U_5 \\ U_6 \\ U_7 \\ U_8 \\ \cdot \\ \cdot \end{Bmatrix} = \begin{Bmatrix} F_1 \\ F_1 \\ F_2 \\ F_2 \\ F_3 \\ F_3 \\ F_4 \\ F_4 \\ \cdot \\ \cdot \end{Bmatrix}$$

where:

k_n = a component in the global stiffness matrix

U_n = a component in the global displacement vector

F_n = a component in the global force vector.

The boundary conditions imposed on the above system of equations are as follows. For the rigidly fixed nodal points,

$$U_1 = U_3 = U_5 = U_7 = \ldots = U_{2n-1} = 0 \qquad (2.10)$$

and for the nodal points that move in unison,

$$U_2 = U_4 = U_6 = U_8 = \ldots = U_{2n} \quad . \qquad (2.11)$$

The system of equations of equation (2.9) with the boundary conditions of (2.10) and (2.11) applied were solved for nodal point displacements using IMSL math library subroutine DLSARG.

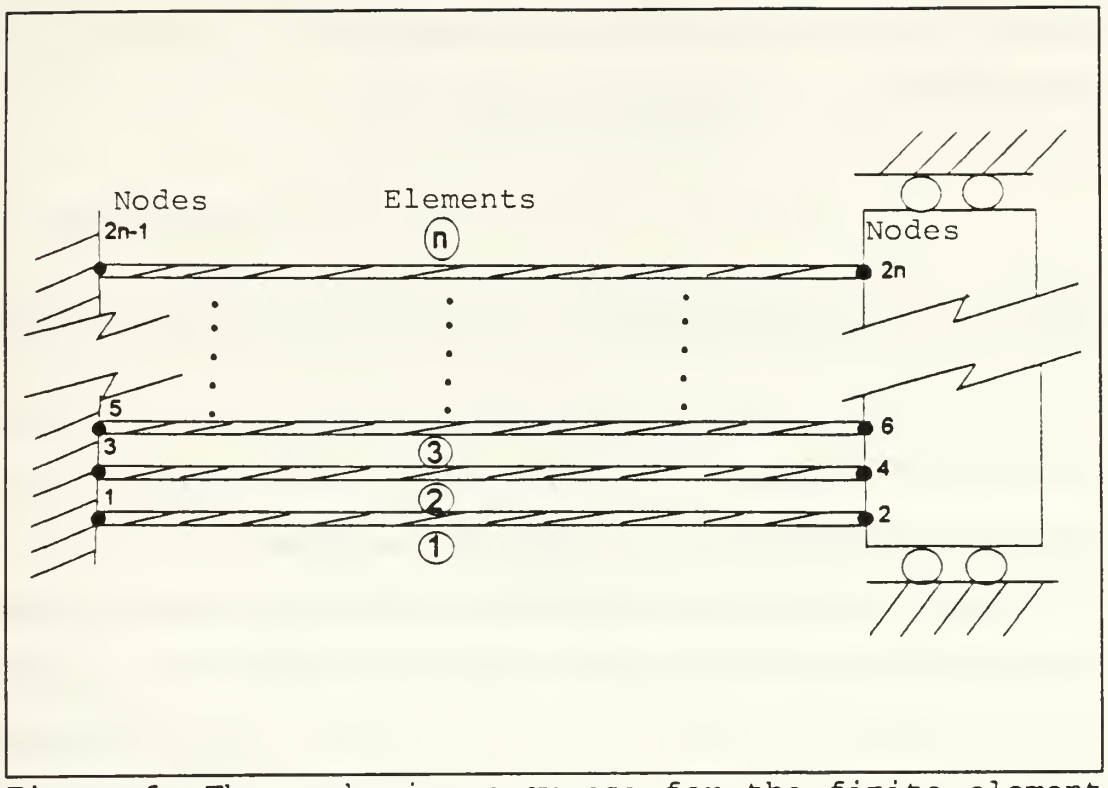

Figure 6: The numbering sequence for the finite element solution.

The stresses of the fibers per ply were calculated using the displacements obtained from the above system of equations as follows (see figure 4):

$$\epsilon_a = \epsilon_m + \epsilon_{th} \tag{2.12}$$

$$\epsilon_m = \epsilon_a - \epsilon_{th}$$

where

ϵ_a = strain from actual motion of nodal points=$(u_2-u_1)/L$

ϵ_m = strain causing fiber stress

ϵ_{th} = fiber strain for free expansion=$\alpha(T-T_\infty)$.

Substitution of appropriate expressions for ϵ_a and ϵ_{th} gives an expression for mechanical strain of:

$$\epsilon_m = \epsilon_a - \epsilon_{th} = \left\{ \frac{(u_2 - u_1)}{L} - \alpha (T - T_\infty) \right\} \quad . \tag{2.13}$$

Finally multiplying equation (2.13) by Young's modulus yields:

$$\sigma = E\epsilon_m = E\left\{ \frac{(u_2 - u_1)}{L} - \alpha (T - T_\infty) \right\} \tag{2.14}$$

where σ is the stress developed in the fiber.

Using the preceding equations a computer stress program was developed utilizing the Vatikiotis combustion code for fiber temperature profiles. The stress program determined fiber stresses throughout the composite material as a function of time and location. The stress program also determined failed fibers based on failure criteria of Chapter III. Specifics of the stress program are contained in Chapter IV.

III. FAILURE CRITERIA

A. INTRODUCTION

The stress analysis code determines fiber stresses throughout the composite plate and then determines if failure of any of the fibers has occurred. In this chapter possible fiber failure criteria are considered. The four failure modes considered were tensile strength failure, compressive strength failure, fiber buckling, and fiber consumption. Of the four modes considered only three were incorporated in the stress analysis code.

B. TENSILE FAILURE

The first criteria considered was failure due to exceeding the fibers tensile strength of 300 ksi. When subjected to heat graphite fibers tend to contract, which is reflected in their thermal expansion coefficient of $-0.55X10^{-6}/^{o}F$. Initially, the fiber closest to the heat source will increase in temperature then over time the remaining fibers will heat. The plate fibers will continue to rise in temperature as long as the heat source is applied. Since thermal strain is proportional to temperature, the magnitude of fiber contraction increases with fiber temperature. Due to the fibers closest to the fire being hotter than those further from the fire, fibers closest to the fire would, if free to do

so, contract more than those farther away. This variation in tendency to contract causes induced stresses since all fibers are restrained to contract uniformly as seen in Figure 4.

In order to estimate the temperature required to reach tensile strength, a limiting case of Equation (2.14) was used. Since the fiber closest to the heat source is the first to heat, its temperature begins to rise before any significant change in the other fiber temperatures. As a worst case, this fiber could be heated to a very high temperature while all the remaining fibers remained very close to their initial temperature. If the number of fibers were relatively high, this situation could be modeled as one heated fiber with fixed ends (i.e. not allowed to move axially). Using this model equation (2.14) becomes:

$$S_t = -E\alpha\,(T-T_\infty) \tag{3.1}$$

or, by rearranging, the minimum temperature required for this fiber to reach the tensile strength is:

$$T_{min} = \frac{S_t}{-E\alpha} + T_\infty \tag{3.2}$$

where:

S_t = tensile strength of the fiber (300 ksi)

T_{min} = the minimum temperature for tensile failure

E = elastic modulus (31.0×10^6 psi)

T_∞ = reference temperature (assumed to be 60°F)

α = thermal expansion coefficient ($-0.55 \times 10^{-6}/^\circ$F).

Solving the above equation for the minimum fiber temperature gives a value of approximately 17,600°F. This temperature is unachievable since graphites melting point is approximately 6000°F and, moreover, the combustion code is unable track temperatures over approximately 2600°F.

Due to the above calculation, the probability of any fibers failing in the tensile mode is highly unlikely. However, a quick check for tensile failure was incorporated into the computer program as verification of the above calculations. Tensile failure was not observed during any of the case studies.

C. COMPRESSIVE STRENGTH FAILURE

The next criteria considered was purely axial compression of the fibers. For the graphite fibers under consideration their compressive strength is 260 ksi. However, this high value is quite deceiving. These fibers have a very small cross section and relatively long length, causing them to be susceptible to buckling failure when in compression. Stresses at buckling are much lower than the compressive fracture strength. For this reason compressive strength of the fibers was not used as a failure criteria.

D. FIBER BUCKLING

The third failure mode considered was fiber buckling. The graphite fibers have a very high slenderness ratio due to

their small cross sectional diameter and relatively long length. These fibers could be susceptible to Euler column buckling. Evaluation of this mode of failure requires a "typical" length for the unsupported fibers. This fiber length was assumed to be 10 inches, corresponding to a reasonable sized hole burned through the material. These fibers were further assumed to have fixed end conditions.

The development of Euler Buckling formula is available in several texts and will not be redeveloped here. From [Ref. 5] the formula for Euler column buckling assuming fixed end conditions with constant circular cross sectional area is:

$$\sigma_{cr} = \frac{\pi^2 E D^2}{4L^2} \qquad (3.3)$$

where:

σ_{cr} = critical stress for column buckling

E = elastic modulus of the fibers

D = the Diameter of the fibers

L = the length of the unsupported fibers.

Using the above formula, the calculated value of σ_{cr} is approximately 19 psi. This value is very small and quite conservative since the model assumes no lateral support.

As the epoxy matrix burns, some of the combustion products will stay behind forming a new matrix material. This new matrix structure consisting of residual combustion products, although weaker than the original epoxy matrix, renders lateral support to the fibers. This additional support

significantly increases the critical buckling strength of the fibers.

Rosen [Ref. 6], in his work on critical buckling stress of composite materials, develops two analytical models for buckling of composites, namely; the extensional mode and the shear mode. Of these two modes, the mode most likely for fiber volume fractions of approximately 20% is the shear mode. The shear mode formula is:

$$\sigma_{fcr} = \frac{G_m}{V_f(1 - V_f)} \tag{3.4}$$

where:

σ_{fcr} = fiber critical buckling stress

V_f = fiber volume fraction

G_m = shear modulus of the matrix material.

A search of literature provided little information on the properties of epoxy combustion products for use as a matrix material. However, after some consideration, this problem was overcome by assuming that the effect of the combustion products, as a matrix material, could be modeled as a small fraction (F) of the original graphite-epoxy composite buckling critical stress given by equation (3.4). This fraction (F) is associated with the amount of lateral support the graphite fibers receive from the combustion products. Using this assumption the following equation was used for fiber buckling criteria,

$$\sigma'_{fcr} = \frac{G_m}{V_f(1 - V_f)} F \qquad (3.5)$$

where σ'_{fcr} is the reduced buckling critical stress and F is the combustion product fraction, that is, the fraction of the original stress due to combustion product lateral support. Failure of the graphite fibers due to exceeding the reduced buckling stress as calculated above is used by the stress analysis program. Different values of the combustion product fraction (F) are assumed to assess the effect of this fraction on failure.

E. FIBER CONSUMPTION

Fiber consumption was considered as the last failure mode. As the plate burns, under some conditions, the supply of oxygen in the interior of the plate becomes depleted. At that time the burning process moves to the X=0 surface where the air is being drawn into the plate. From then on the plate continues to burn at the surface of the plate slowly decreasing in thickness as the temperature profile across the plate tends to a constant value. This mode of burning is surface recession.

The relatively constant temperature profile produced across the plate in the surface recession mode, could reduce the stresses seen by the fibers. If these stresses are small

in magnitude, the possibility of fiber failure by consumption is possible. Surface recession fiber consumption was incorporated into the stress analysis code to eliminate burnt away fibers from the analysis.

IV. COMPUTER PROGRAMS

A. MODIFICATIONS TO THE COMBUSTION CODE

Only superficial modifications were made to Vatikiotis' combustion code for this study. First, the computer code was brought up to Fortran 77 language by changing a few read and write format statements. Second, a single statement reading numerous input variables from the input file was broken up into individual read statements in order to facilitate an easy to read comment type input file format. This input file containing a short description of each input variable is contained in Appendix D. Third, a few output statements were added to facilitate building output data files for use in the stress analysis. The fourth and final change to this program was to increase the number of nodal points so that the present program could handle up to 101 nodal points vice the older 31 nodal points. Increases in computer speed along with significant memory resources over the past few years facilitated this change. The amount of accuracy was significantly improved by using a larger number of nodal points, as seen in both Figure 8 and Table 1. Both display the same typical run of the combustion code varying only the number of nodal points used. Temperatures at the locations of X=0" (the fire surface), X=0.25" (half the medium thickness),

and X=0.5" (the surface opposite the fire) are compared. As seen, previous models of the program were not grid independent for the X=0" location.

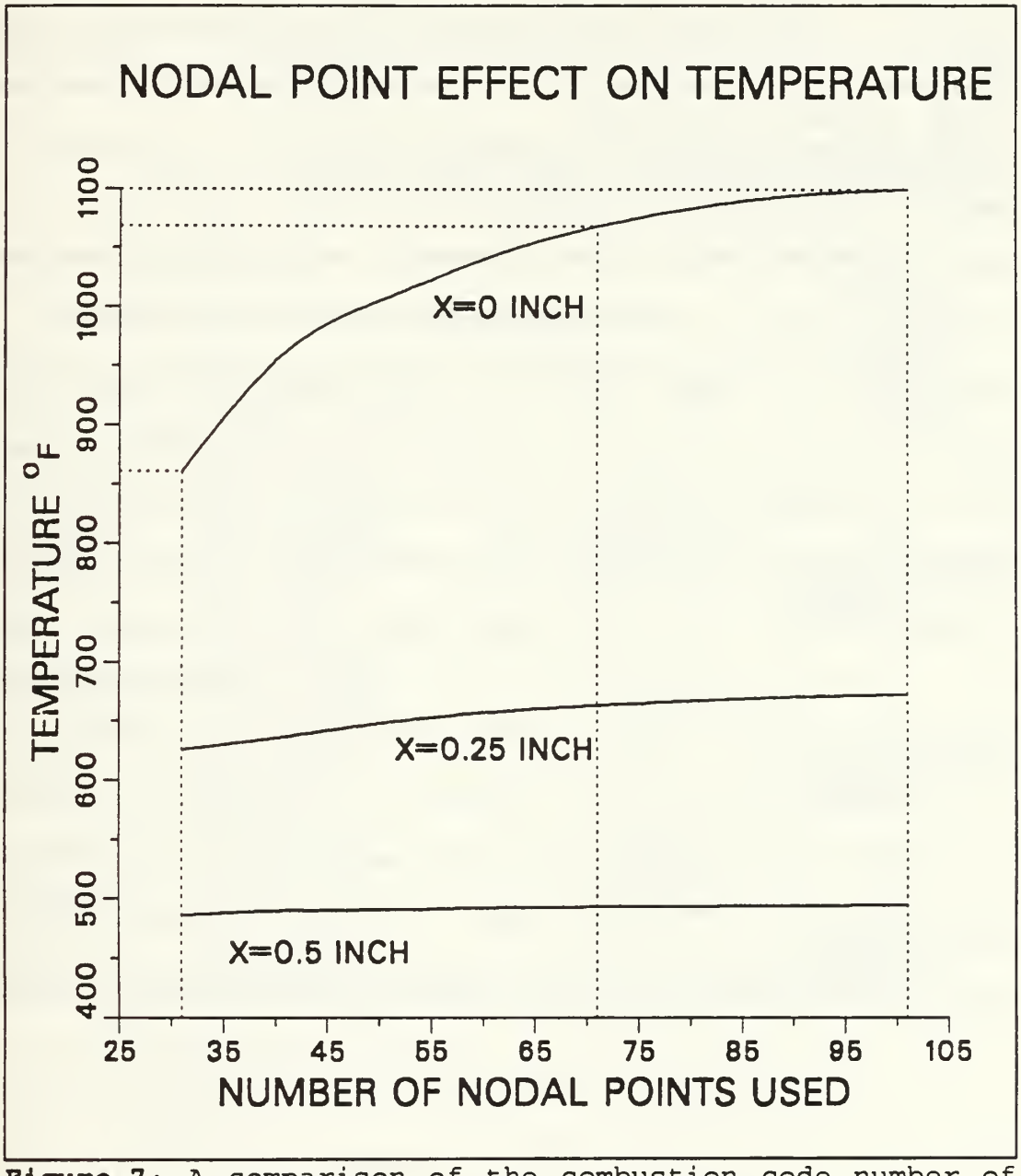

Figure 7: A comparison of the combustion code number of nodal points and calculated temperature.

TABLE 1: INCREMENTAL TEMPERATURE CHANGE VERSUS NODAL POINTS USED.

TIME OF RUN: 60 seconds
HEAT FLUX APPLIED: 10,000 BTU/ft^2 hr
DIFFERENTIAL PRESSURE ACROSS THE MEDIUM: 0.8 psi
MEDIUM THICKNESS: 0.5 inches

NUMBER OF NODAL POINTS USED	GRAPHITE TEMPERATURE °F AT LOCATION		
	X=0 inch	X=0.25 inch	X=0.5 inch
30	822.46	607.35	486.48
31	860.57	625.83	486.23
INCREMENTAL CHANGE	4.4%	3.0%	0.05%
70	1066.23	662.77	493.31
71	1068.11	662.77	493.14
INCREMENTAL CHANGE	0.2%	0.02%	0.03%
100	1099.51	672.21	494.42
101	1100.33	672.43	494.54
INCREMENTAL CHANGE	0.07%	0.03%	0.02%

B. STRESS ANALYSIS PROGRAM

The stress program, as shown in Figure 8, obtains temperature information from an output data file produced by Vatikiotis' combustion code. Location data from the combustion code was presented in normalized (X/L) form since the equations Vatikiotis used were non-dimensionalized. In the stress code these locations were converted into absolute location points (X). Until burn off of the fibers starts (i.e. prior to surface recession) the non dimensionalized locations (X/L) remain fixed. However, when surface recession starts, combustion moves to the X=0 surface and the thickness of the material decreases with time. As the thickness of the material changes the stress code continually verifies stress code fiber locations removing burned away fibers from the stress analysis.

Vatikiotis in his combustion code formulation used a method of "smearing" to account for both the fiber and air filled void as shown in Figure 9. Denoting the porosity of the medium as p, we have $dV_a=pdV$ and $dV_g=(1-p)dV$ where dV is the total differential volume of air and graphite fiber, dV_a is the differential volume of air and dV_g is the differential volume of graphite. The effect of this smearing process is to replace individual fibers and voids, which are extremely large in number, by a homogenous material. This process is utilized in the basic differential equations presented in Appendix A.

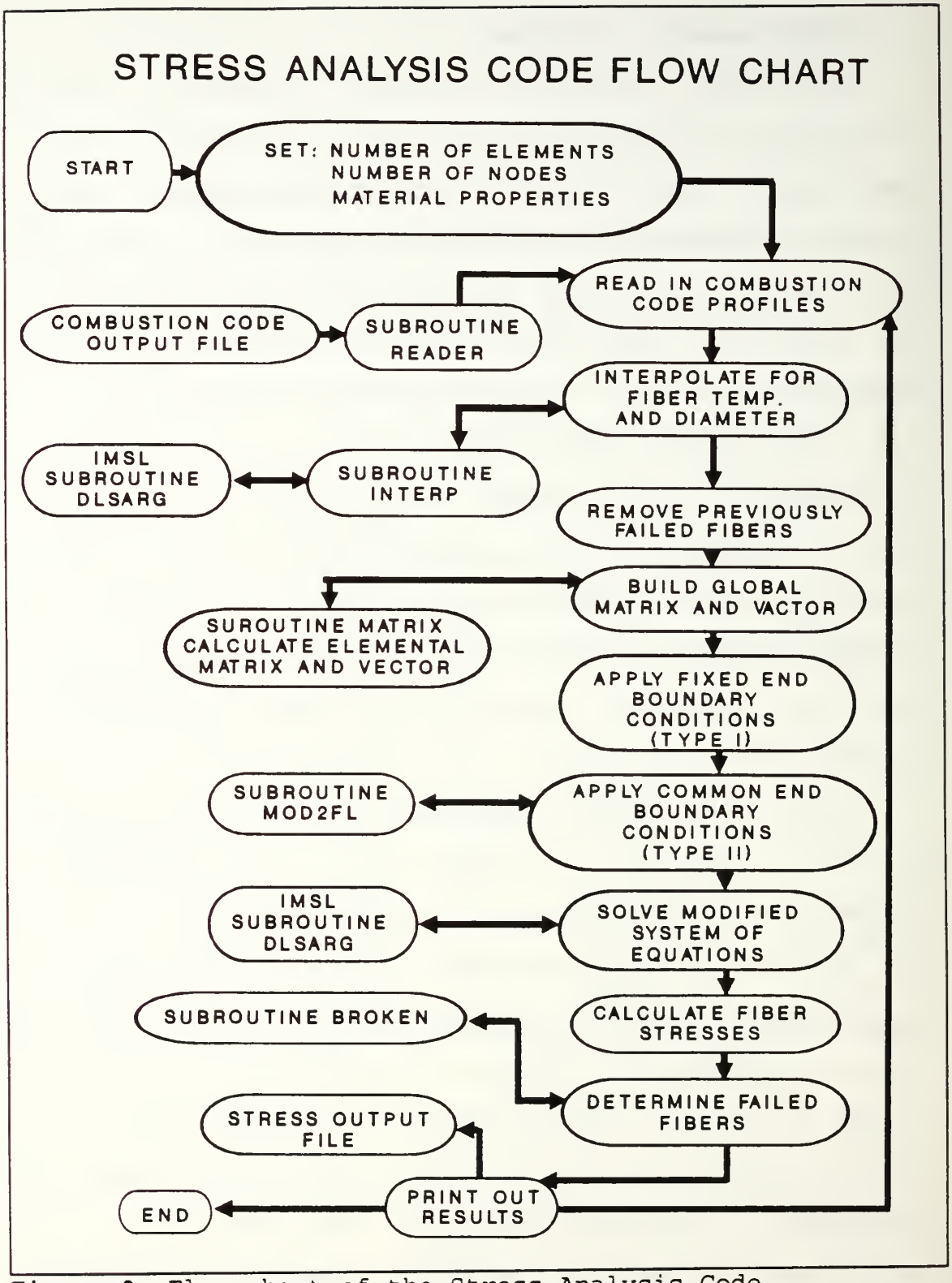

Figure 8: Flow chart of the Stress Analysis Code.

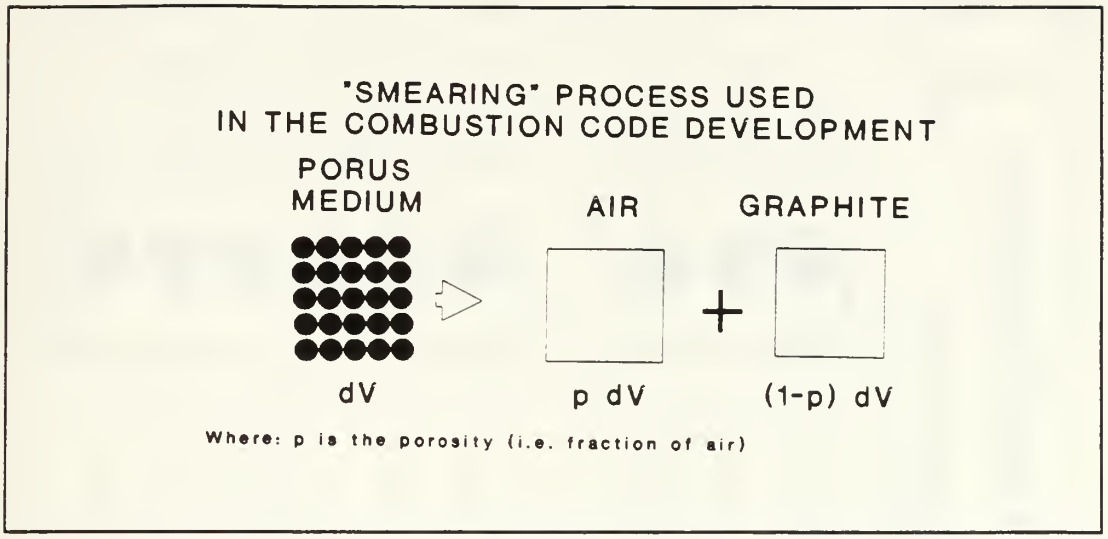

Figure 9: The process of "smearing" used in the combustion code.

The stress code accommodated the idea of a homogeneous material and utilized temperature output by the following procedure (see Figure 10). First the graphite temperatures along with nodal point locations are determined from the combustion code. These combustion code locations are compared to the center location of each ply. When the ply center location is bracketed by the combustion code locations the stress code performs quadratic interpolation to determine the graphite fiber temperature for that ply. By this method, accurate temperature profiles can be obtained from the combustion code using 101 nodal points while at the same time the number fibers used in the stress code may be varied.

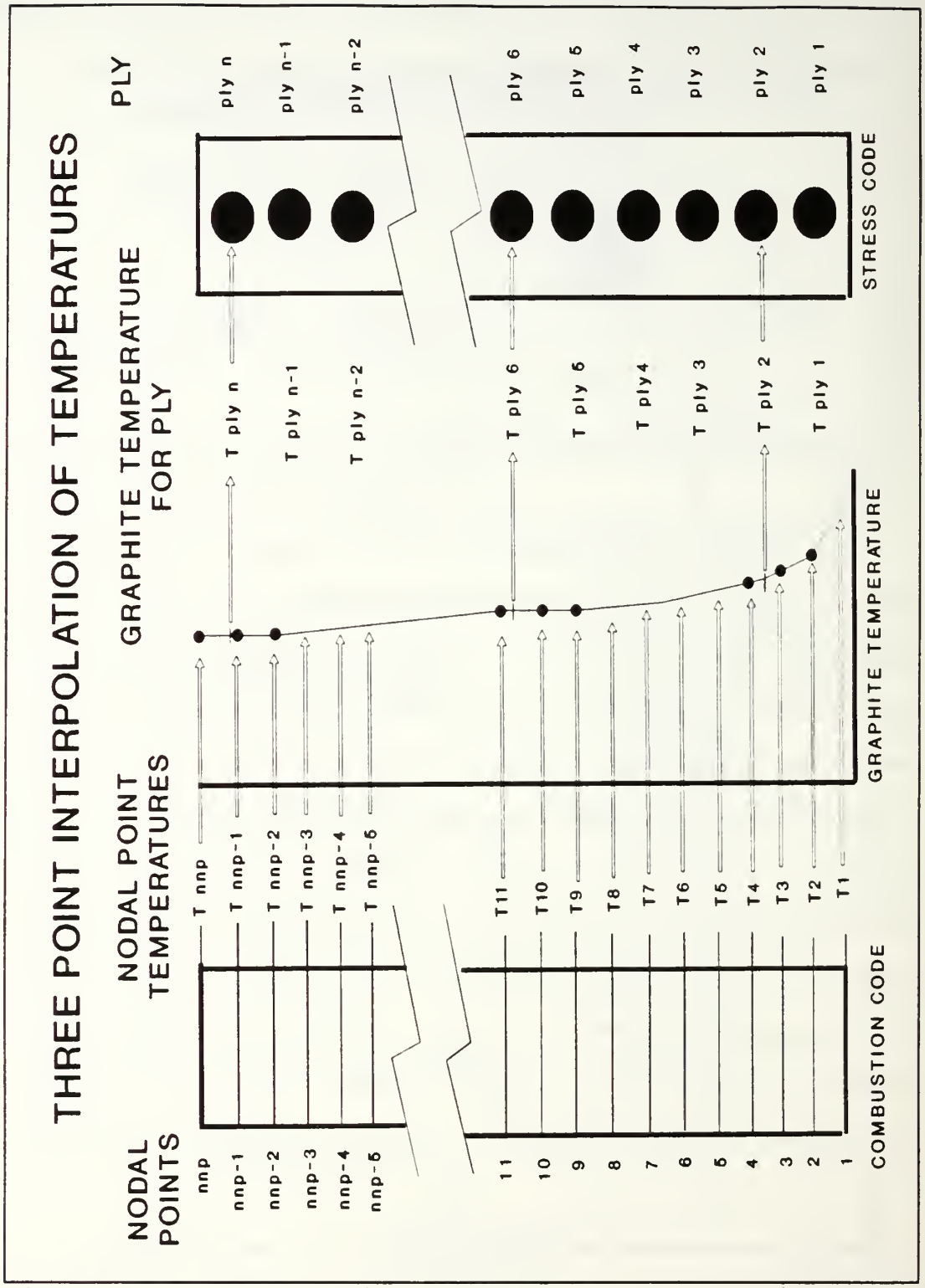

Figure 10: Interpolation method from combustion code temperatures to stress code temperatures.

Elemental matrix equations are determined using Equation (2.8). These elemental matrices are assembled into a global set of equations of the general form:

$$\begin{array}{c} \\ 1 \\ \vdots \\ j \\ \vdots \\ k \\ \vdots \\ m \end{array} \begin{array}{c} \begin{array}{cccccc} 1 & \cdots & j & \cdots & k & \cdots & m \end{array} \\ \begin{bmatrix} K_{11} & \cdots & K_{1j} & \cdots & K_{1k} & \cdots & K_{1m} \\ \vdots & & \vdots & & \vdots & & \vdots \\ K_{j1} & \cdots & K_{jj} & \cdots & K_{jk} & \cdots & K_{jm} \\ \vdots & & \vdots & & \vdots & & \vdots \\ K_{k1} & \cdots & K_{kj} & \cdots & K_{kk} & \cdots & K_{km} \\ \vdots & & \vdots & & \vdots & & \vdots \\ K_{m1} & \cdots & K_{mj} & \cdots & K_{mk} & \cdots & K_{mm} \end{bmatrix} \end{array} \begin{Bmatrix} U_1 \\ \vdots \\ U_j \\ \vdots \\ U_k \\ \vdots \\ U_m \end{Bmatrix} = \begin{Bmatrix} F_1 \\ \vdots \\ F_j \\ \vdots \\ F_k \\ \vdots \\ F_m \end{Bmatrix} \qquad (4.1)$$

where:

K = the global stiffness matrix

U = the global displacement vector

F = the global force vector

m = the total number of nodal points (2n)

j and k = are arbitrary integers where $1 \leq j$ and $k \leq m$.

The boundary conditions imposed on this matrix equation (4.1), fit two different forms; Type I and Type II. Their application is performed as follows. The Type I boundary conditions consist of those that fit the form:

$$U_j = b \qquad (4.2)$$

where:

U_j = displacement at node j,

b = a known constant.

This type of boundary condition is directly comparable to the fixed end of the fibers (i.e. the locations of all the odd numbered nodal points) where b=0. Applying a single boundary condition, U_j=b to the equation set (4.1) above gives the following modified matrix equation:

$$\begin{array}{c} \\ 1 \\ \vdots \\ j \\ \vdots \\ k \\ \vdots \\ m \end{array} \begin{array}{c} \begin{array}{cccccccc} 1 & \cdots & j & \cdots & k & \cdots & m \end{array} \\ \downarrow \\ \begin{bmatrix} K_{11} & \cdots & 0 & \cdots & K_{1k} & \cdots & K_{1m} \\ \vdots & & \vdots & & \vdots & & \vdots \\ 0 & \cdots & 1 & \cdots & 0 & \cdots & 0 \\ \vdots & & \vdots & & \vdots & & \vdots \\ K_{k1} & \cdots & 0 & \cdots & K_{kk} & \cdots & K_{km} \\ \vdots & & \vdots & & \vdots & & \vdots \\ K_{m1} & \cdots & 0 & \cdots & K_{mk} & \cdots & K_{mm} \end{bmatrix} \end{array} \begin{Bmatrix} U_1 \\ \vdots \\ U_j \\ \vdots \\ U_k \\ \vdots \\ U_m \end{Bmatrix} = \begin{Bmatrix} F_1 - bK_{1j} \\ \vdots \\ b \\ \vdots \\ F_k - bK_{kj} \\ \vdots \\ F_m - bK_{mj} \end{Bmatrix} . \quad (4.3)$$

The stress code was written to apply each fixed end boundary condition using the same method as (4.3) above.

The Type II boundary conditions fit the form of:

$$U_j + aU_k = c \qquad (4.4)$$

where:

U_j and U_k = are two degrees of freedom

a = known constant

c = known constant.

Application of the general boundary condition of Equation(4.4) to the matrix Equation (4.1) above yields:

(4.5)

$$
\begin{array}{c}
\\
1 \\
\vdots \\
j \rightarrow \\
\vdots \\
k \rightarrow \\
\vdots \\
m
\end{array}
\begin{array}{c}
\begin{array}{ccccccc} 1 & & j & \cdots & k & \cdots & m \\ & & \downarrow & & \downarrow & & \end{array} \\
\begin{bmatrix}
K_{11} & \cdots & 0 & \cdots & (K_{1k}-aK_{1j}) & \cdots & K_{1m} \\
\vdots & & \vdots & & \vdots & & \vdots \\
0 & \cdots & 1 & \cdots & +a & \cdots & 0 \\
\vdots & & \vdots & & \vdots & & \vdots \\
(K_{k1}-aK_{j1}) & \cdots & +a & \cdots & (K_{kk}-2aK_{jk}+a^2K_{jj}+a^2) & \cdots & (K_{km}-aK_{jm}) \\
\vdots & & \vdots & & \vdots & & \vdots \\
K_{m1} & \cdots & 0 & \cdots & (K_{mk}-aK_{mj}) & \cdots & K_{mm}
\end{bmatrix}
\end{array}
\begin{Bmatrix} U_1 \\ \vdots \\ U_j \\ \vdots \\ U_k \\ \vdots \\ U_m \end{Bmatrix}
=
\begin{Bmatrix} F_1-cS_{ij} \\ \vdots \\ c \\ \vdots \\ F_k-aF_j-cK_{kj}+acK_{jj}+ac \\ \vdots \\ F_m-cK_{mj} \end{Bmatrix}
$$

The detail for developing this modified matrix equation is given by Akin [Ref. 8].

The Type II boundary condition of equation (4.2) above is directly relatable to the fiber ends that move in unison,

$$
\begin{aligned}
U_2 + (-1)\,U_4 &= 0 \\
U_4 + (-1)\,U_6 &= 0 \\
U_6 + (-1)\,U_8 &= 0 \\
&\vdots \\
U_{2n-2} + (-1)\,U_{2n} &= 0
\end{aligned}
\qquad (4.6)
$$

with a=-1 and c=0. The Type II boundary conditions of Equation (4.6) were applied in the stress analysis program.

The final system of equations with both sets of boundary conditions applied was solved for the displacement vector U using the IMSL library subroutine DLSARG.

Once nodal point displacements U_j(j=1,2...,2n) were known fiber stresses σ were determined using equation (2.14). This process was continued for each time step of output data

obtained from the combustion code. The fiber stress analysis code is included in Appendix B.

V. CASE STUDIES

The combustion code requires input data to start the analysis. Several input data files were produced encompassing various combinations of composite thickness, heat flux, differential pressure and combustion product fraction (F). Specific values of these variable parameters as used in the case studies are listed in Table 2. Several other important parameters were treated as constants for these studies as listed in Table 3. The input data files required by the combustion code were built covering all 1008 combinations of the variable parameters. These data files were processed by the combustion code and then the temperature profile data was further processed for stress failure information. Most of the lower heat flux results, primarily below 4000 btu/ hr-ft^2, produced relatively minor increases in plate temperatures which resulted in insignificant stresses and no failure. But the majority of runs gave interesting results. The final results of this effort are provided in graphical form in the following case studies.

TABLE 2: THE PARAMETERS VARIED IN THE CASE STUDIES.

INPUT PARAMETERS THAT WERE VARIED FOR THE CASE STUDIES WITH THE VALUES INVESTIGATED
COMPOSITE THICKNESS: 0.25", 0.5",0.75", 1.0"
CONSTANT HEAT FLUX (thousand btu/hr-ft^2): 1, 1.25, 1.5, 1.75, 2, 2.5, 3, 3.5, 4.0, 4.5, 5, 5.5, 6, 6.5, 7, 7.5, 8, 8.5, 9, 10, 25
DIFFERENTIAL PRESSURE (psi): 0.05, 0.5, 0.7
COMBUSTION PRODUCT FRACTION (%): 1, 0.75, 0.5, 0.25

TABLE 3: PARAMETERS TREATED AS CONSTANT FOR THESE STUDIES.

CONSTANT INPUT PARAMETERS TO THE COMBUSTION CODE FOR THE CASE STUDIES
AMBIENT AIR TEMPERATURE: 80°F
AMBIENT AIR PRESSURE: 2116.8 lb/ft^2
TORTUOSITY: 1.4
PARTICLE SHAPE FACTOR: .91
ORDER OF THE CHEMICAL REACTION: 0.5
TIME STEP (between combustion code profiles): 0.5 seconds
STOICHIOMETRIC RATIO: 0.375

A. TEMPERATURE PROFILES

As stated in previously, induced stresses are dependent upon the fiber temperatures. Figures 11 through 16 show the temperature profiles of some representative combustion code runs up to the point of initial fiber failure. Note that the maximum temperature is always at the bottom of the plate where the heat flux is being applied and the air is coming in, while the cooler fibers are at the opposite surface. The main concept to bare in mind for these studies is that graphite fibers contract upon heating, so the hotter fibers will be in a tensile mode (see Figure 4). Since the tensile strength of these hot fibers is very high, these fibers will not fail. However, the fibers that are cooler will be in a compression mode with a low critical buckling strength and they will fail by buckling.

A comparison of Figures 11, 12, and 13 show the effect of increasing the heat flux on a constant thickness material. Notice that for the lower heat fluxes, the temperatures are lower and the profile is more gradual. This, of course, is due to the lower heat flux applied but also due to the ability of the air flow to convectively transfer the heat away from the heated surface. If the heat flux is low, the flow of air through the medium has more time to distribute the heat through the material before failure occurs. If the heat flux

is high, the surface temperature rises quickly and heating is confined primarily to the area close to the heated surface.

A comparison of Figures 11 and 16 indicates the changes in the temperature profile when the highest and lowest differential pressures are applied for a given heat flux and material thickness. As stated previously, the convective heat transfer in the medium has a large effect on the temperature profiles for the lower heat fluxes. For a constant thickness, the pressure gradient $\Delta P/L$ will be higher for a higher differential pressure. This higher pressure gradient causes a higher air flow through the material which increases the convective heat transfer. This increased heat transfer causes both a lower and more gradual temperature profile in the low heat flux cases. However, in the high heat flux cases this effect is insignificant as seen in Figures 12 and 14 for a heat flux of 10,000 btu/hr-ft^2.

As a final comparison Figures 12 and 15 are compared. These figures show the dependence of the temperature profile on thickness of the material while holding differential pressure constant. The temperatures at the surface of the 1.0" plate are higher than the 0.5" plate. This can be explained as follows. If the ΔP is a fixed value, then the thicker plate has a smaller pressure gradient ($\Delta P/L$) because the thickness L is larger. This smaller $\Delta P/L$ gradient will cause less air flow through the thicker material resulting in a lower amount of convective heat transfer. The end result for

the thicker material is a higher and more steep temperature profile. This profile causes more fibers to be in the compressive mode and subsequently fail by buckling.

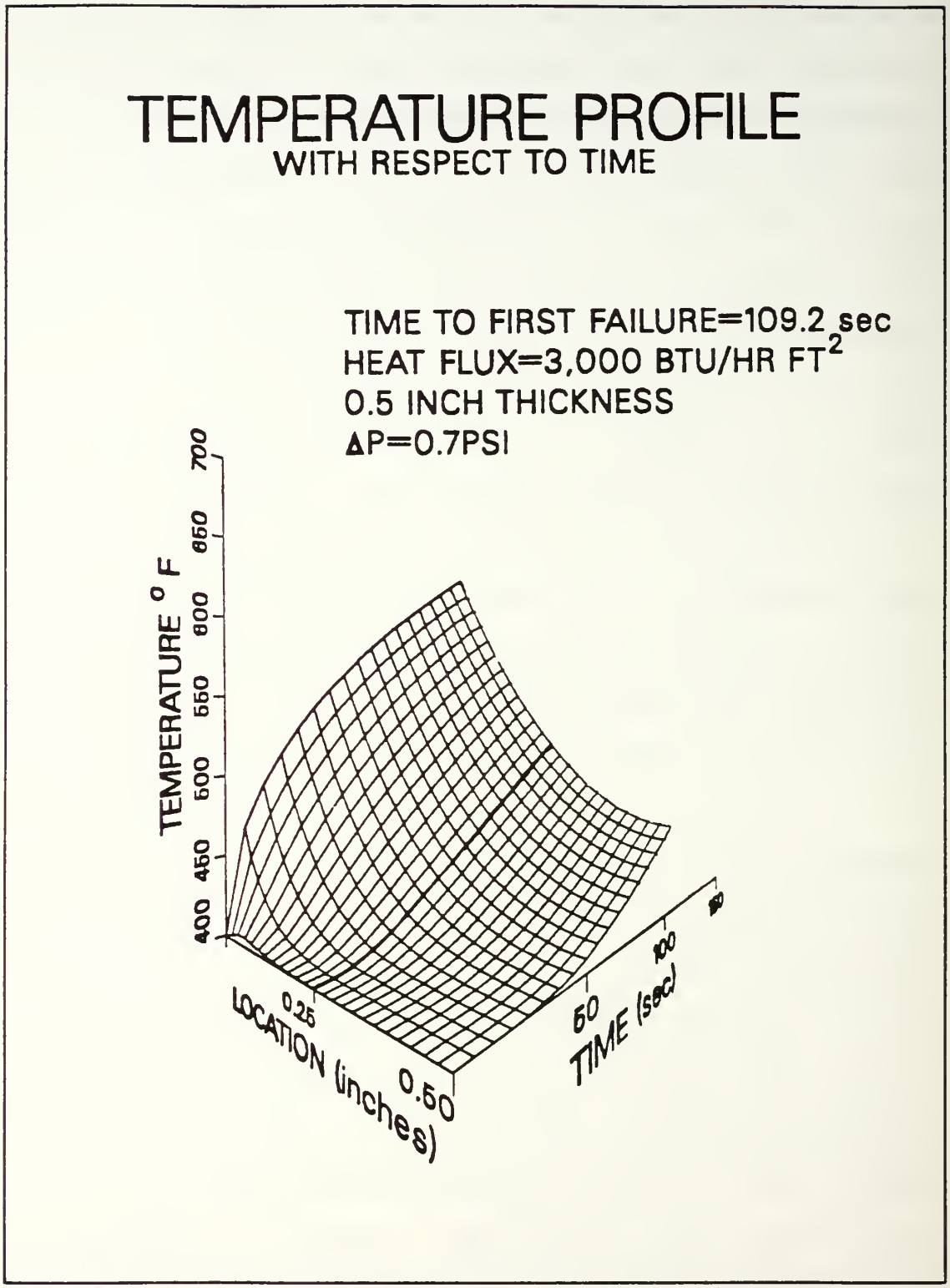

Figure 11: Temperature profile up to first failure for 0.5", 3,000 btu/hr ft^2 and 0.7 psi.

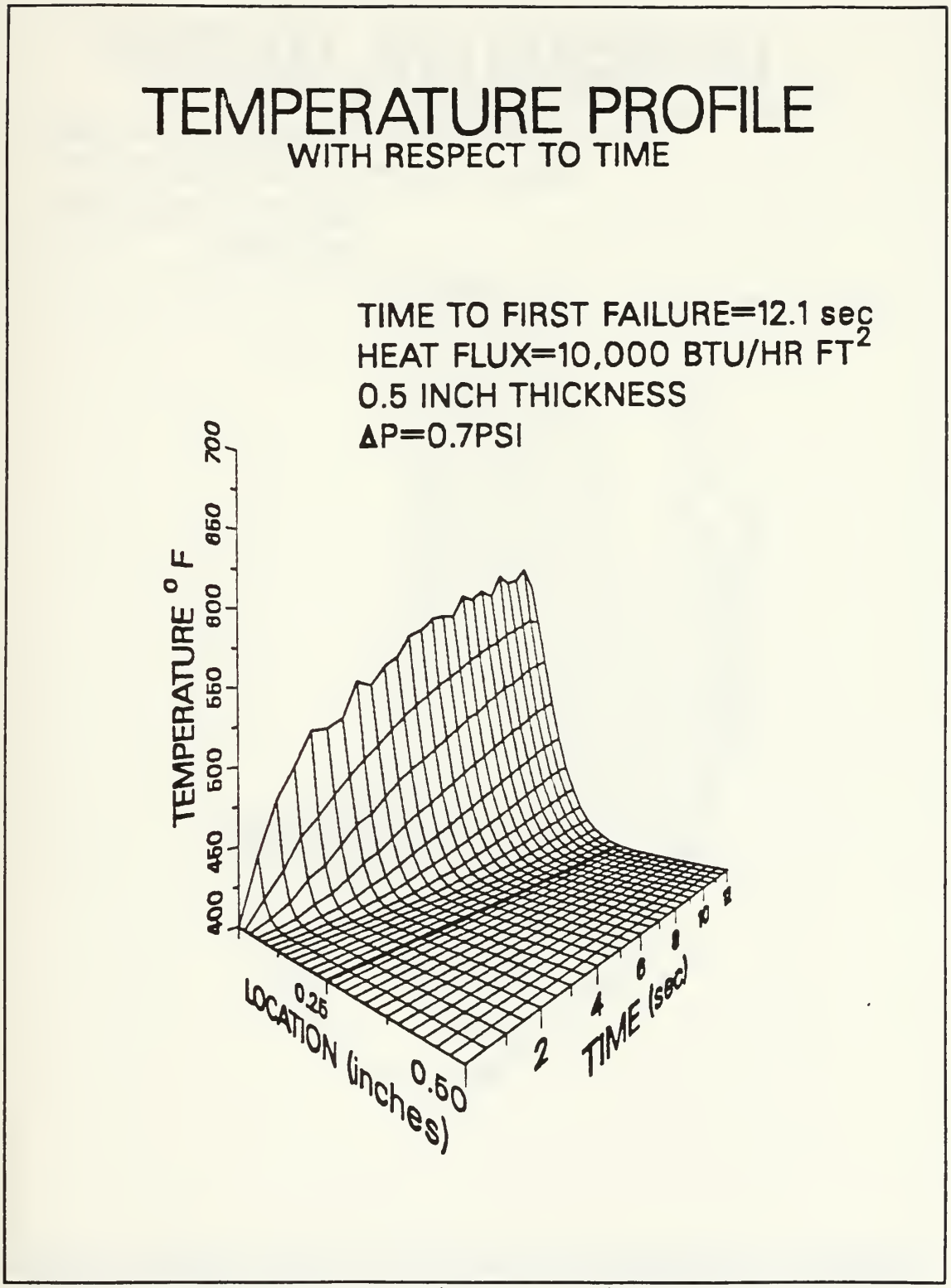

Figure 12: Temperature profile up to first failure for 0.5", 10,000 btu/hr ft^2 and 0.7 psi.

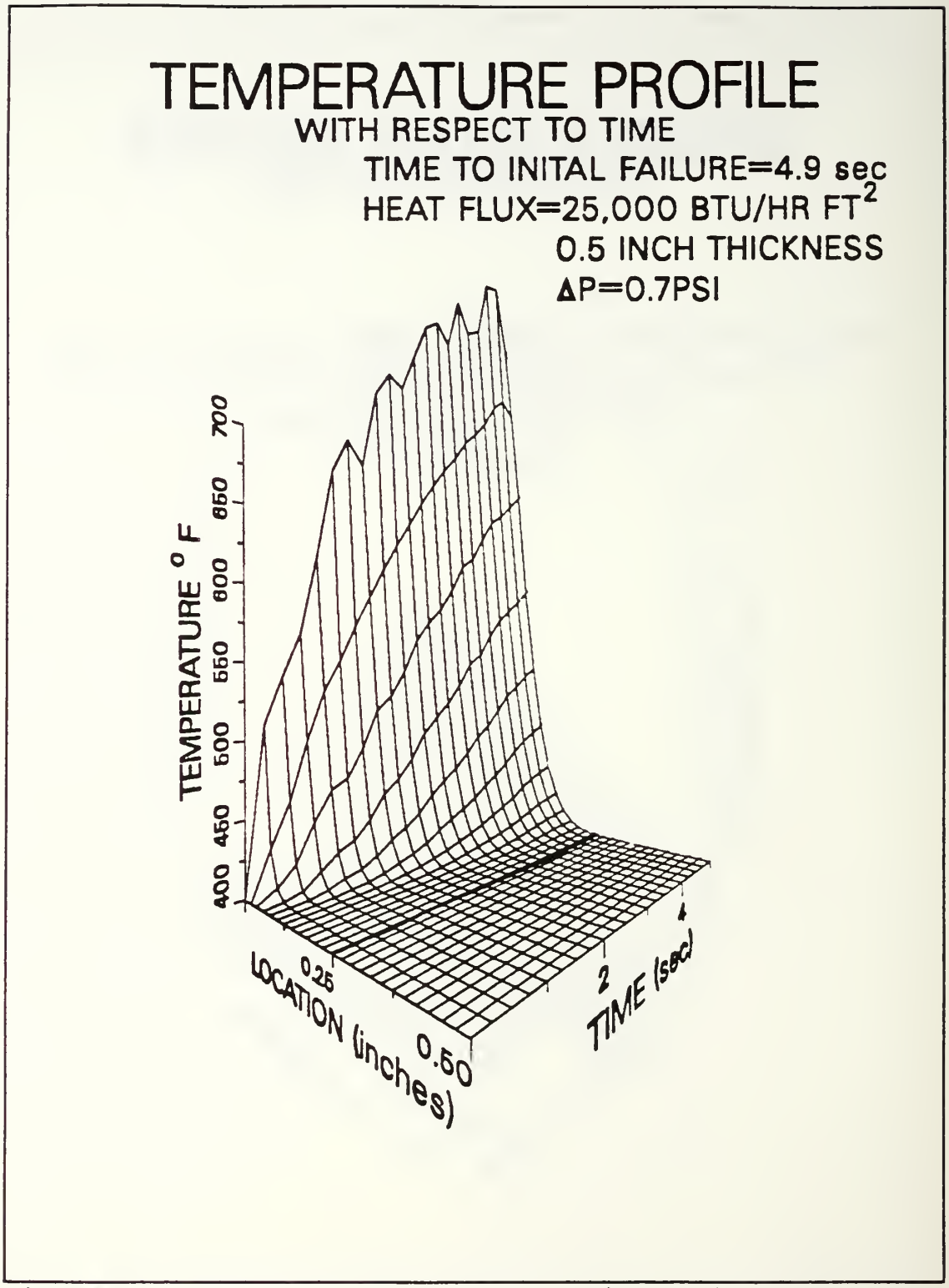

Figure 13: Temperature profile up to first failure for 0.5", 25,000 btu/hr ft^2 and 0.7 psi.

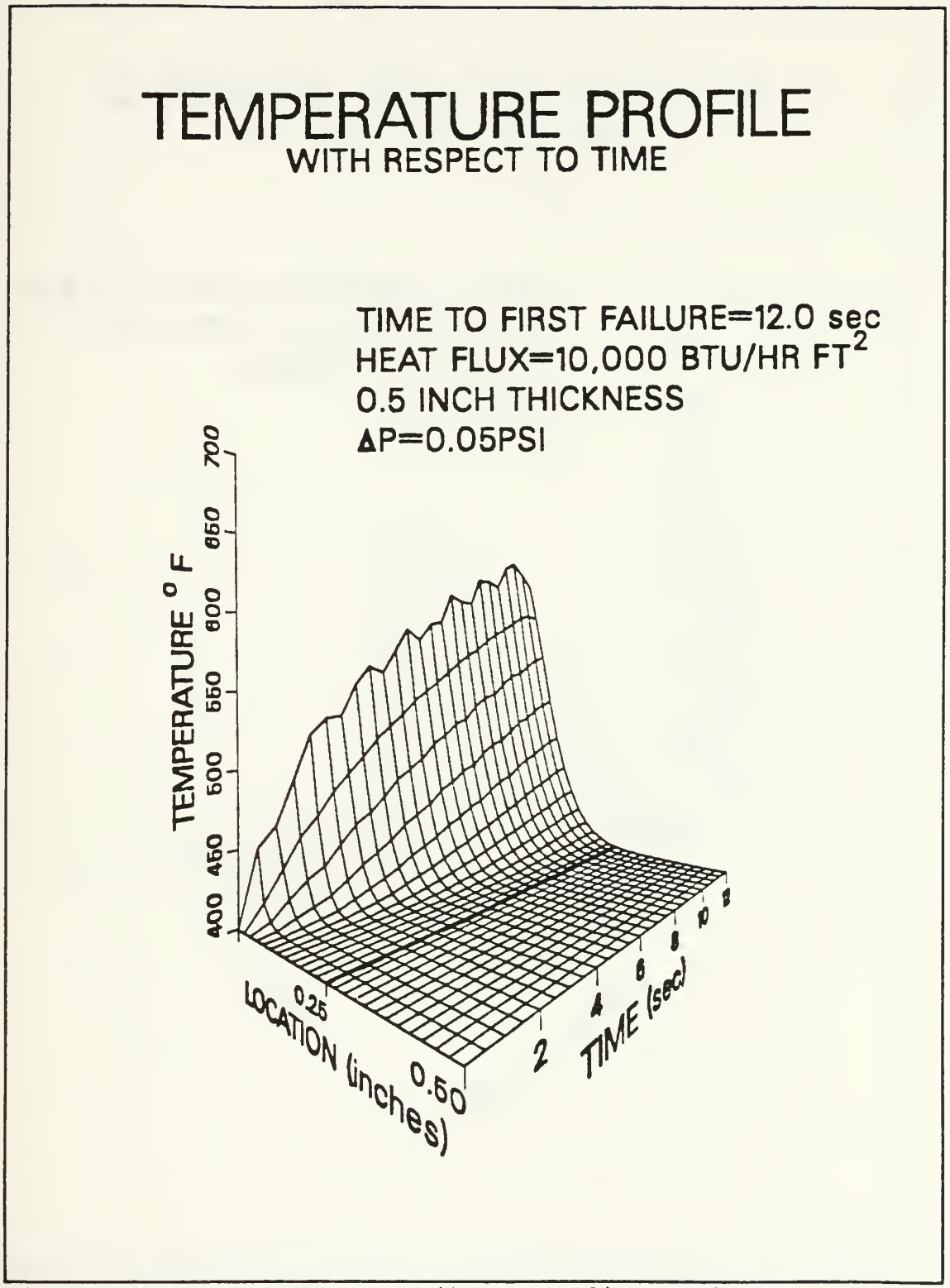

Figure 14: Temperature profile up to first failure for 0.5", 10,000 btu/hr ft^2 and 0.05 psi.

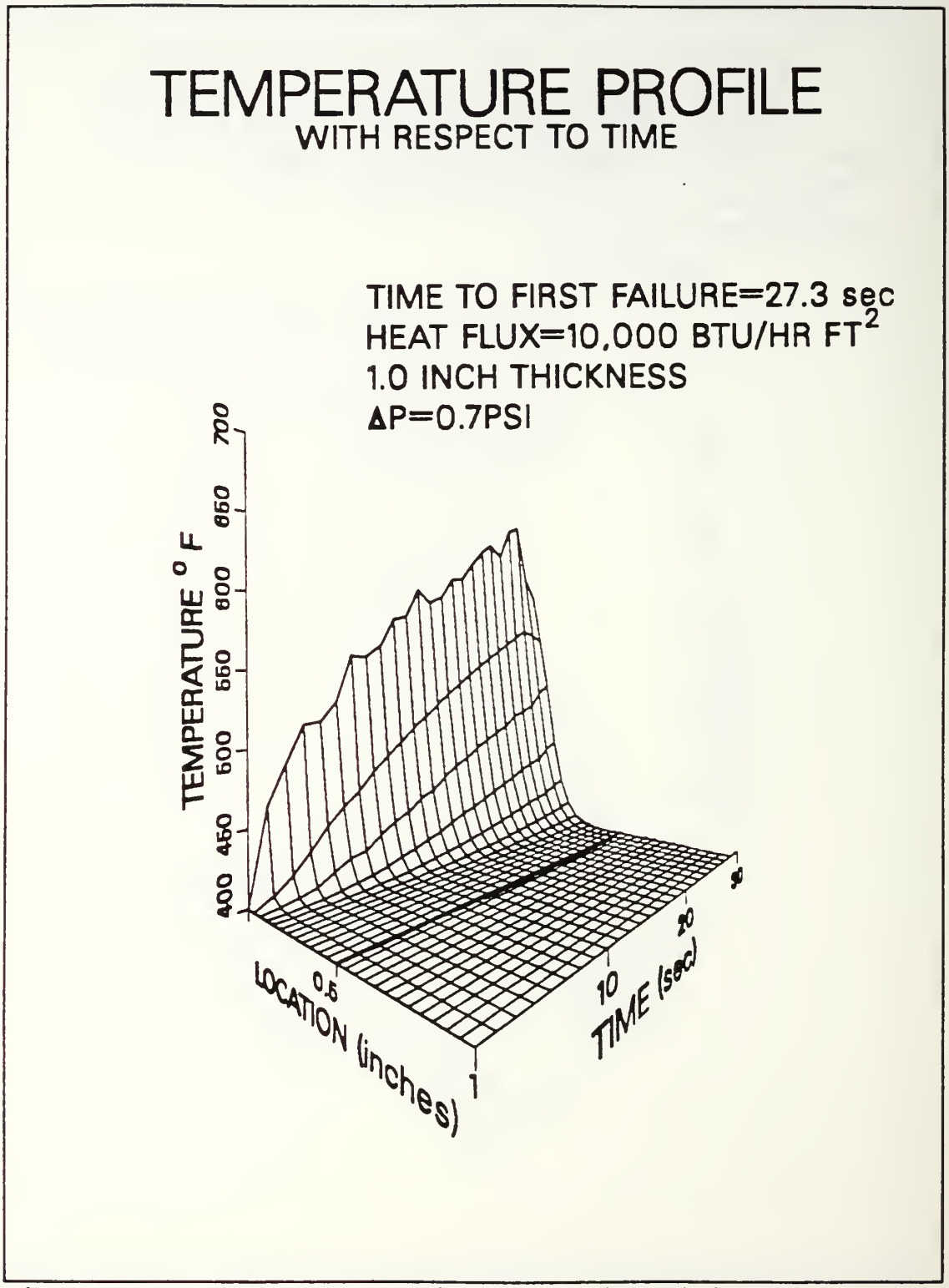

Figure 15: Temperature profile up to first failure for 1.0", 10,000 btu/hr ft^2 and 0.7 psi.

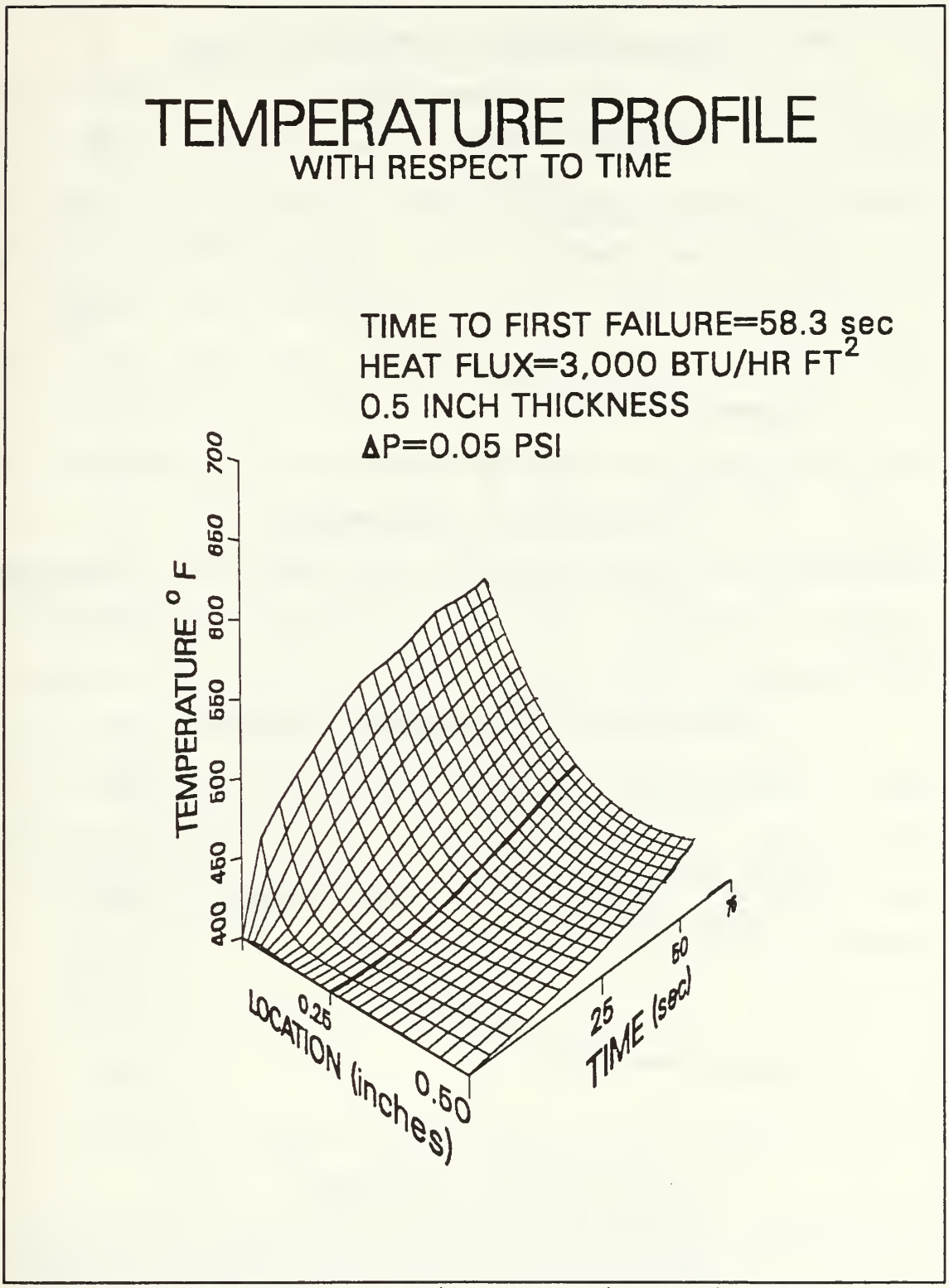

Figure 16: Temperature profile up to first failure for 0.5", 3,000 btu/hr ft^2 and 0.05 psi.

B. TIME TO INITIAL FAILURE (ΔP EFFECT)

Figures 17 through 20 present the time to initial failure showing its dependency on both heat flux and differential pressure. As heat flux decreases, the time to initial failure progressively increases. For each specific ΔP there appears to be a lower bound of heat flux below which failure will never occur. The figures also show that this lower bound value increases with increasing ΔP. However, this lower bound cannot be exactly determined through use of a computer code. Through the use of finite increments of heat flux, given previously in Table 2, this lower bound for failure was roughly determined. As seen in Figures 17 through 20 this lower bound of heat flux was found to within 500 btu/hr-ft^2.

For all thicknesses, the effect of pressure is relatively small except at the lower heat fluxes where the effect of air flow through the material has a large effect on the convective heat transfer. These pressure effects become ineffectual at higher heat fluxes.

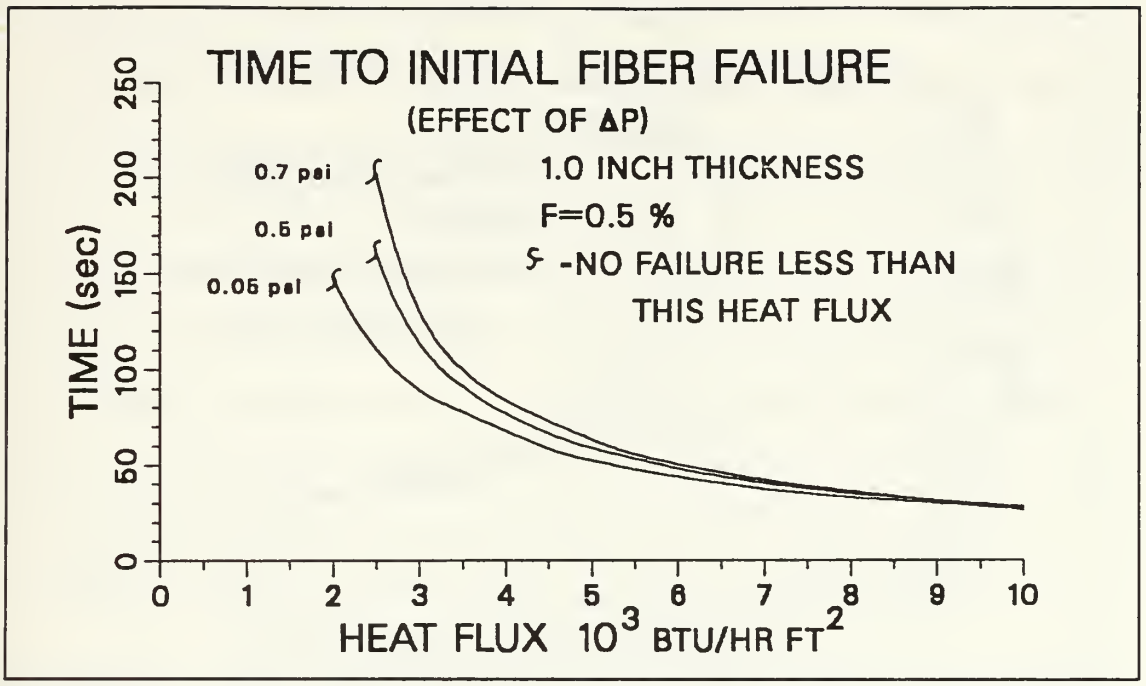

Figure 17: The time to initial failure (effect of differential pressure) for 1.0", and F=0.5%.

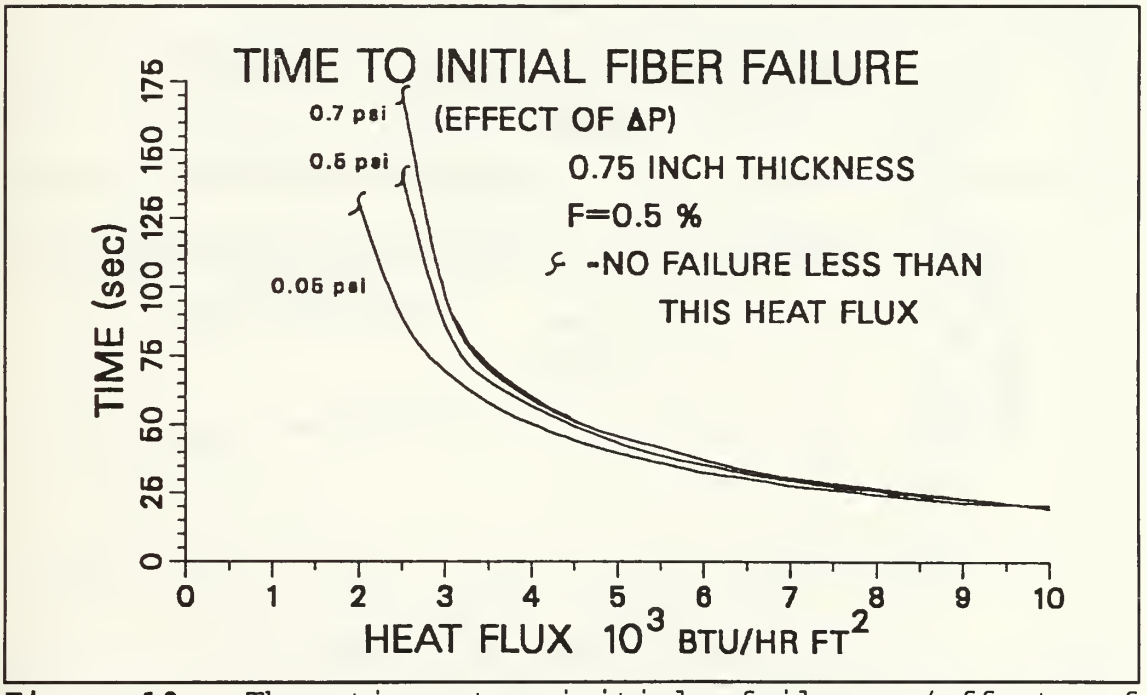

Figure 18: The time to initial failure (effect of differential pressure) for 0.75", and F=0.5%.

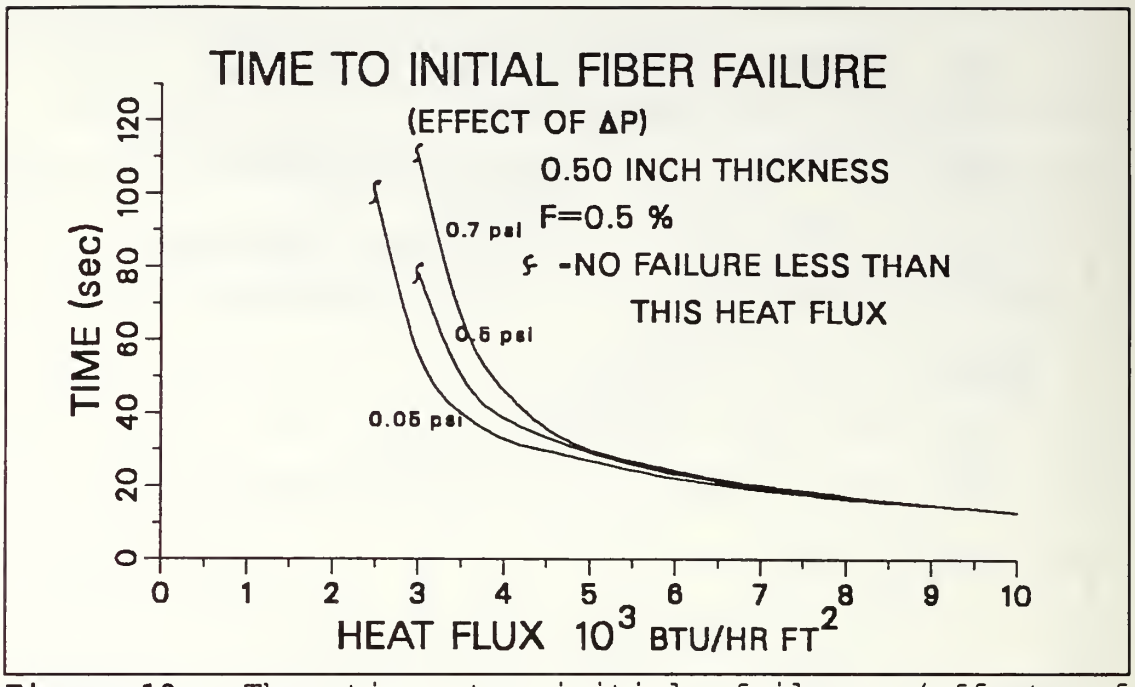

Figure 19: The time to initial failure (effect of differential pressure) for 0.5", and F=0.5%.

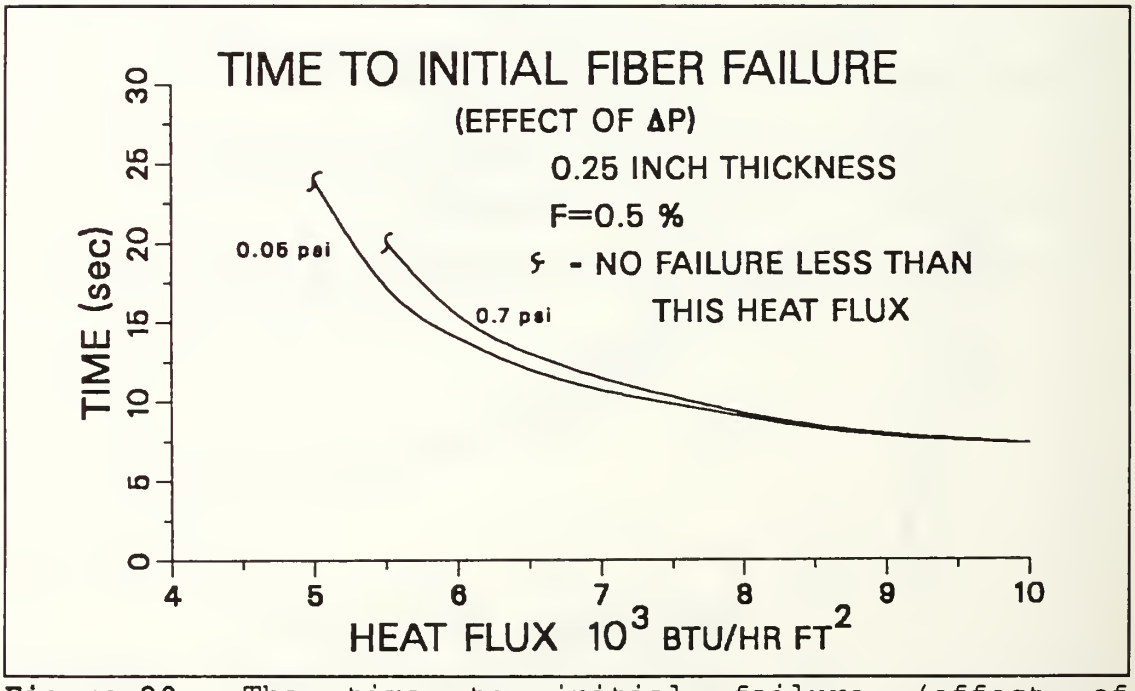

Figure 20: The time to initial failure (effect of differential pressure) for 0.25", and F=0.5%.

C. TIME TO INITIAL FAILURE (F EFFECT)

Figures 21 through 24 demonstrate how the critical buckling strength, and hence time to initial failure, varies with the combustion product factor (F). The value of F greatly effects not only the time to failure but determines whether or not failure will occur. As F increases there is more lateral support for the fibers so the critical buckling strength increases. This increase results in fewer fibers failing by buckling. In the case of the 0.25" plate none of the fibers reached the critical buckling strength when F=1.0%. All figures show that for a given heat flux, as F increases, the time to initial failure increases.

The result of this analysis shows that the value assumed for the combustion product fraction (F) greatly influences the amount of time to initial failure of the material. The figures show that when F increases the resistance to buckling increases and buckling is less likely to occur.

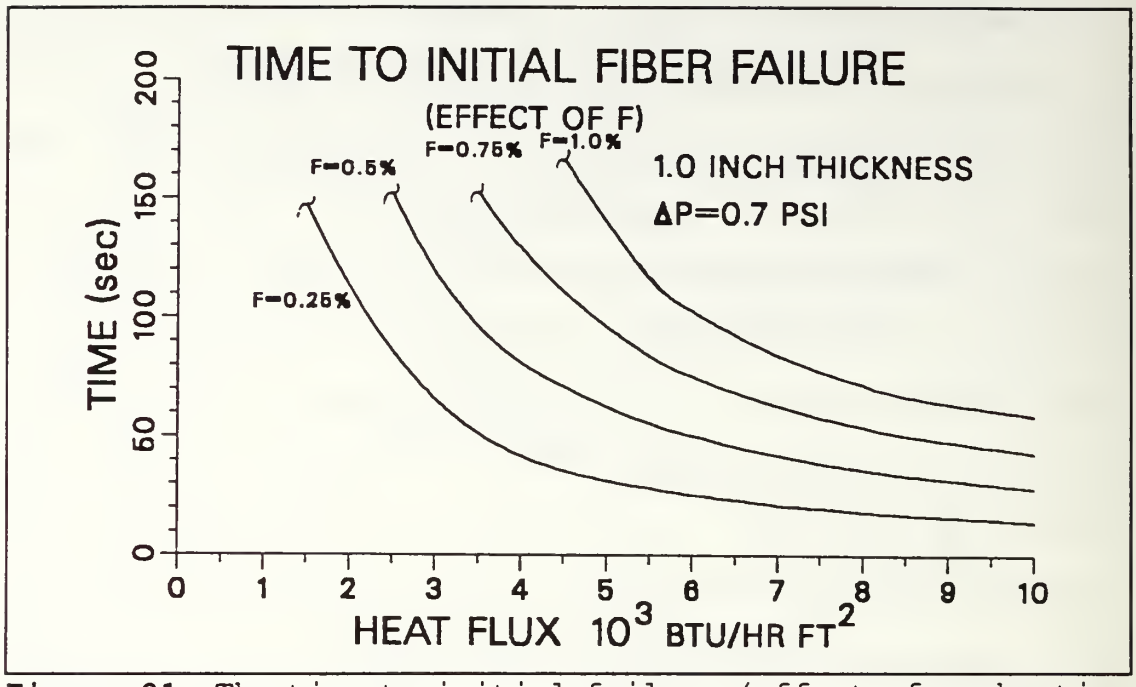

Figure 21: The time to initial failure (effect of combustion product fraction) for 1.0", and ΔP=0.7 psi.

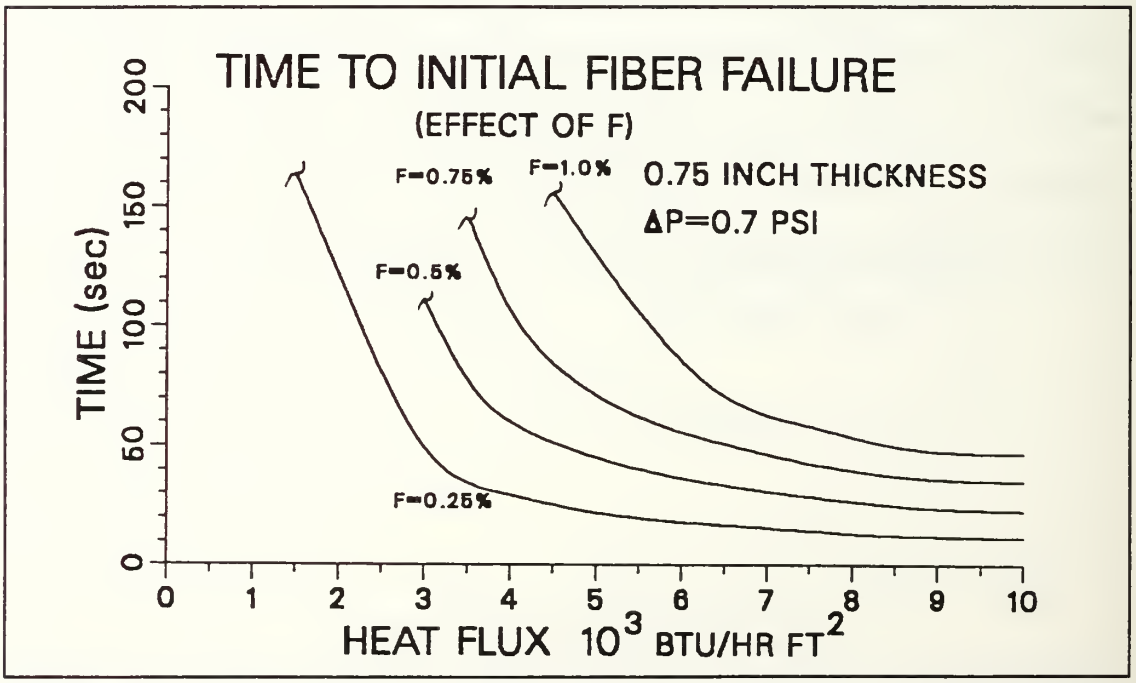

Figure 22: The time to initial failure (effect of combustion product fraction) for 0.75", and ΔP=0.7 psi.

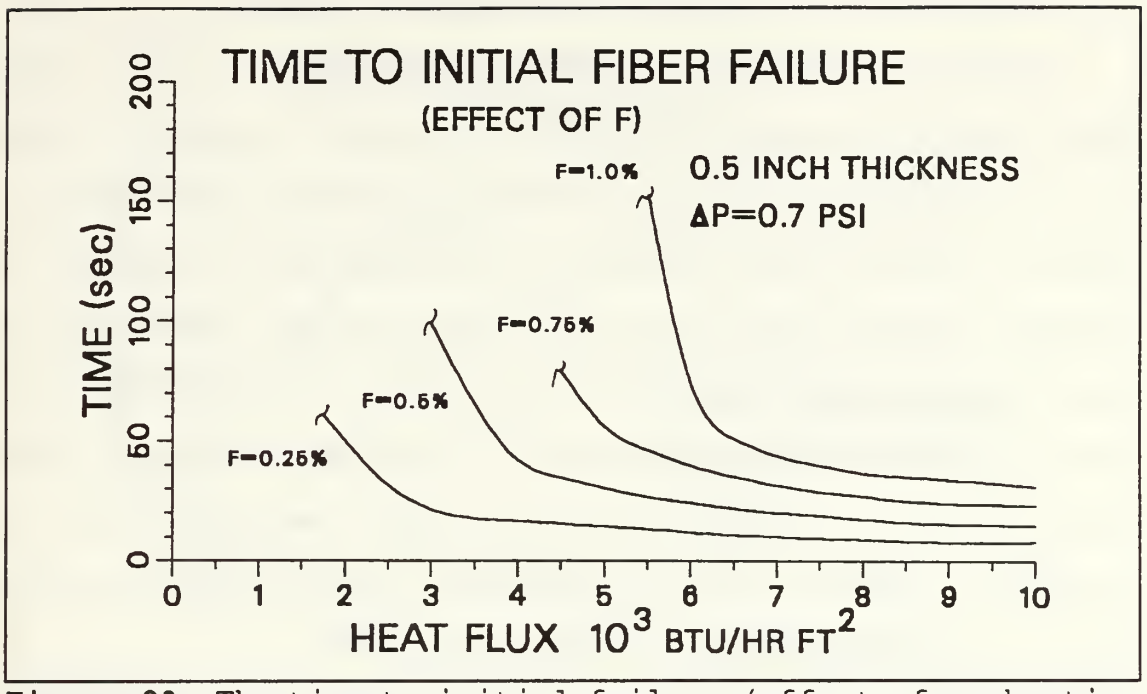

Figure 23: The time to initial failure (effect of combustion product fraction) for 0.5", and ΔP=0.7 psi.

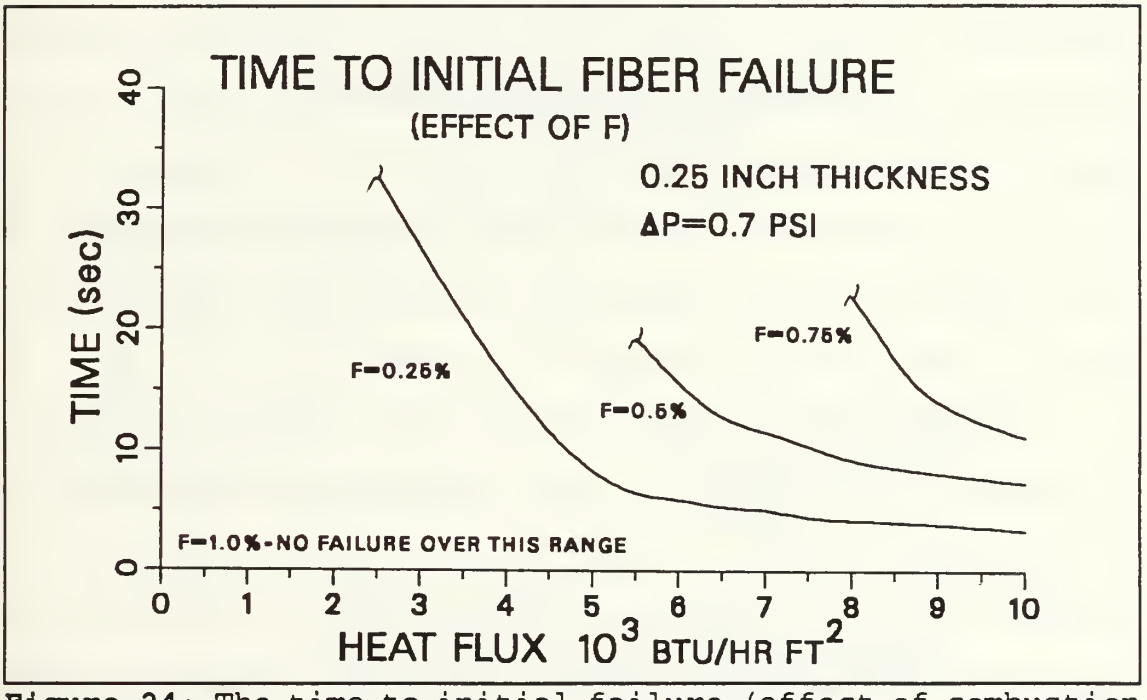

Figure 24: The time to initial failure (effect of combustion product fraction) for 0.25", and ΔP=0.7 psi.

D. PROGRESSION OF MATERIAL FAILURE (ΔP EFFECT)

Figures 25 and 26 track the percentage of failed fibers from the time of the first observed fiber failures. Due to the 0.5 second time step used for temperature profile output, some of these curves start at time zero with a significant number failed fibers. Actually the failure represented by these curves commenced some time between the time of zero of the figures and the previous 0.5 second interval. Since observation of trends in this case are important, the increased computer time to determine a more precise starting time was not justified.

The general trend is, the higher the differential pressure, the lower the percentage of failure. This is apparently is due to the more gradual temperature profiles caused by the higher air flows through the material. For the higher differential pressures/higher air flowrates, more fibers are heated to approximately the same temperature, and are therefore in the tensile mode prior to the time of initial fiber. These tensile fibers do not fail.

Another item worth mentioning is the rapidity of failure. The materials progressed to their maximum percentage of fiber failure very rapidly. For the 1.0" thicker material this maximum failure percentage is reached within 3 seconds of the first fiber failure and for the 0.5" thinner material approximately 4 seconds. These times are independent of differential pressures.

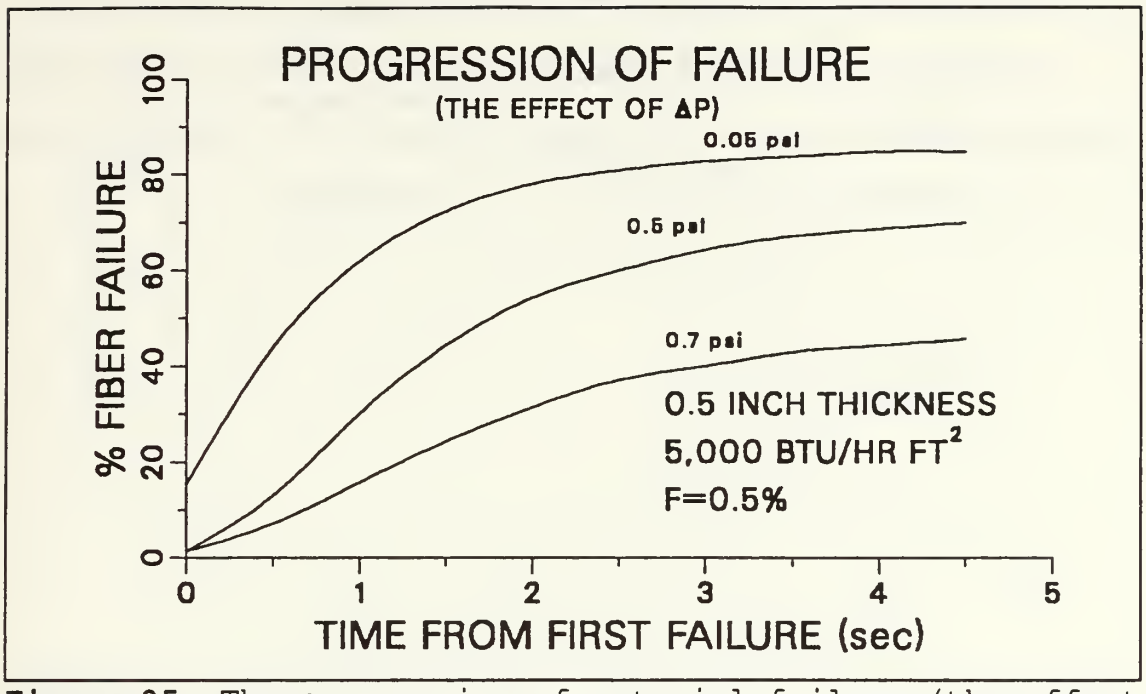

Figure 25: The progression of material failure (the effect of ΔP) for 0.5", and 5,000 btu/ hr-ft^2.

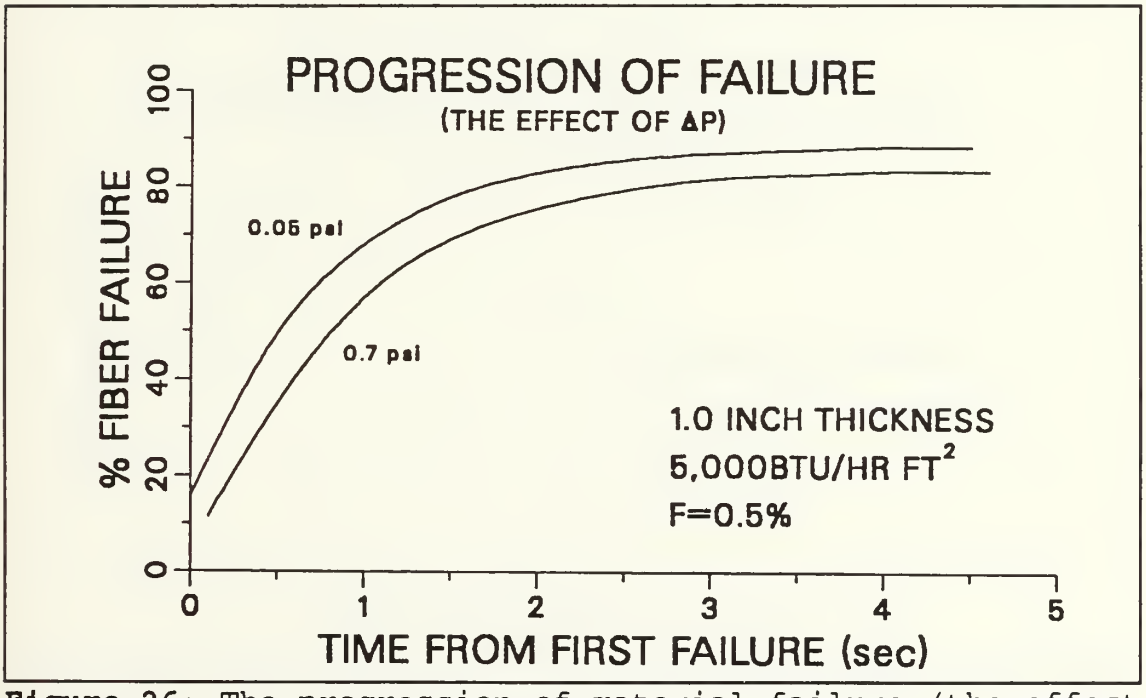

Figure 26: The progression of material failure (the effect of ΔP) for 1.0", and 5,000 btu/hr-ft^2.

E. PROGRESSION OF MATERIAL FAILURE (EFFECT OF HEAT FLUX)

Figures 27 and 28 indicate that as heat flux increases, time to maximum failure changes only marginally, effecting the 3 to 4 second failure time by only 1 second.

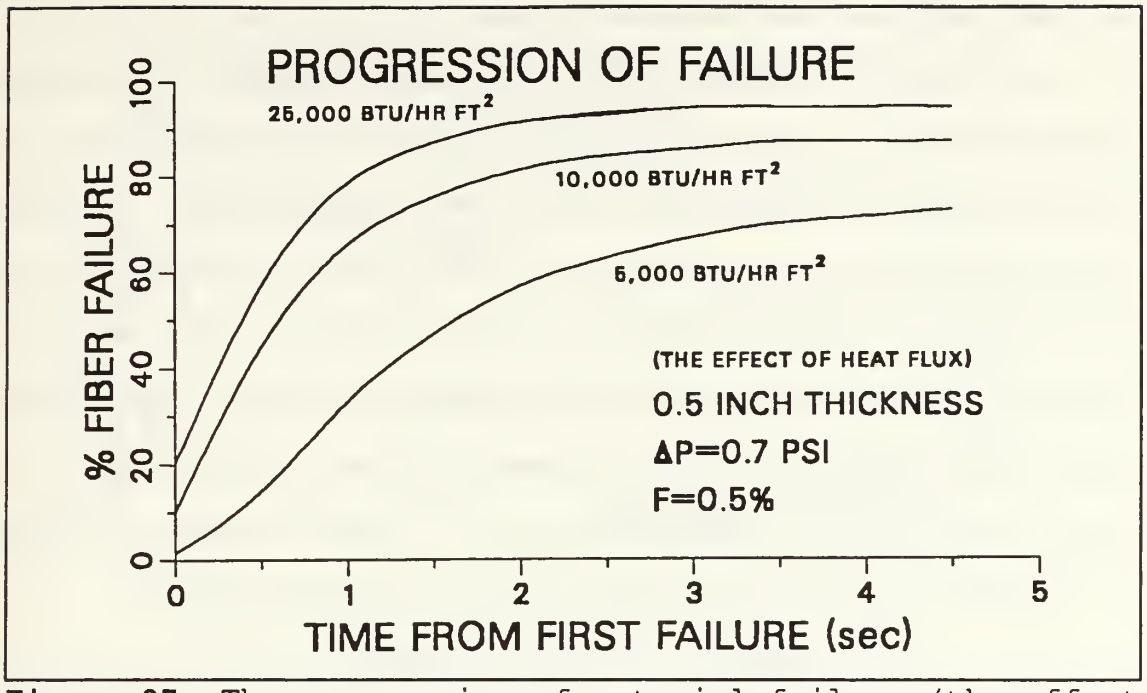

Figure 27: The progression of material failure (the effect of heat flux) for 0.5", and ΔP=0.7 psi.

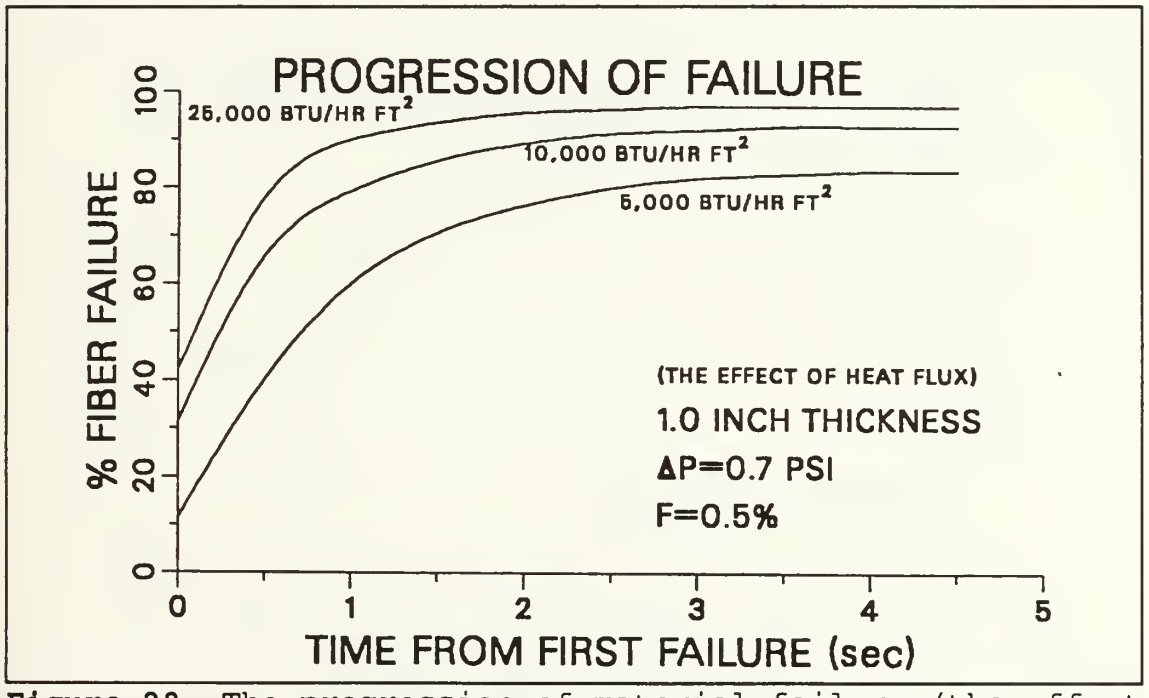

Figure 28: The progression of material failure (the effect of heat flux) for 1.0", and ΔP=0.7.

F. MAXIMUM FAILURE (EFFECT OF ΔP)

Figures 29 through 32 are a consolidation the maximum fiber failure for material failure. These maximum percentages varied slightly with pressure at lower heat fluxes. As shown, for a given material thickness, higher heat fluxes give higher percentage of failed fibers. This is due to the more non-uniform temperature profile discussed previously. The maximum percentage failure seen in these studies is the case of the one inch plate at 25,000 btu/hr-ft^2, which reached a maximum of 97.5%.

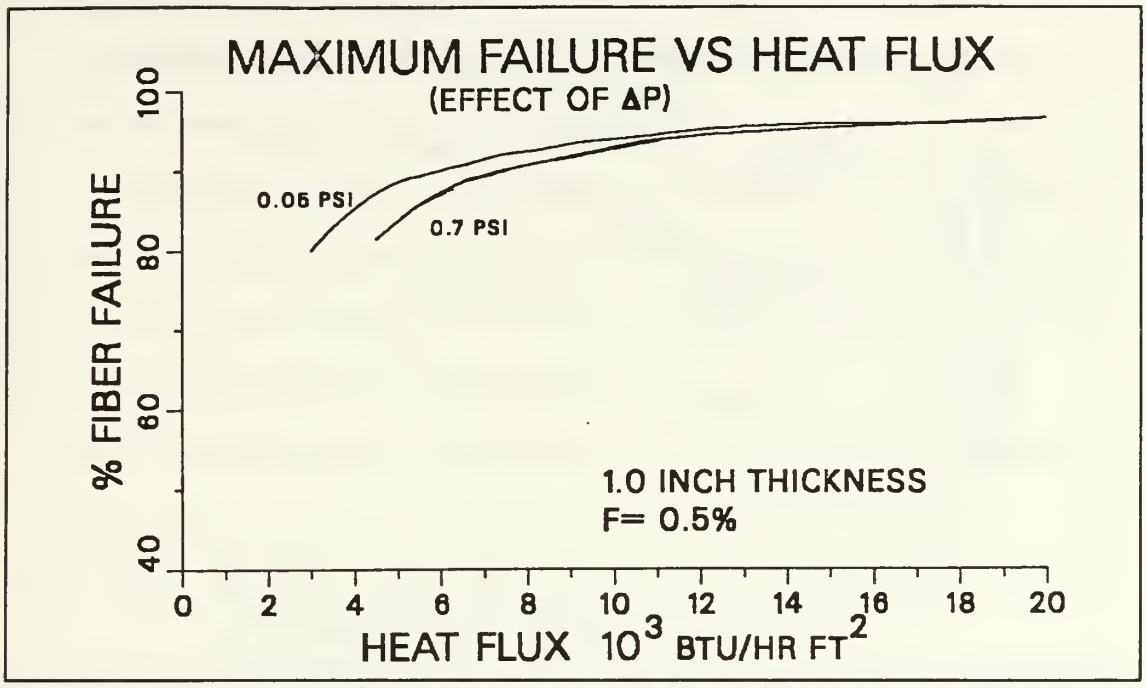

Figure 29: The maximum percentage of failure (the effect of ΔP) for 1.0", and F=0.5%.

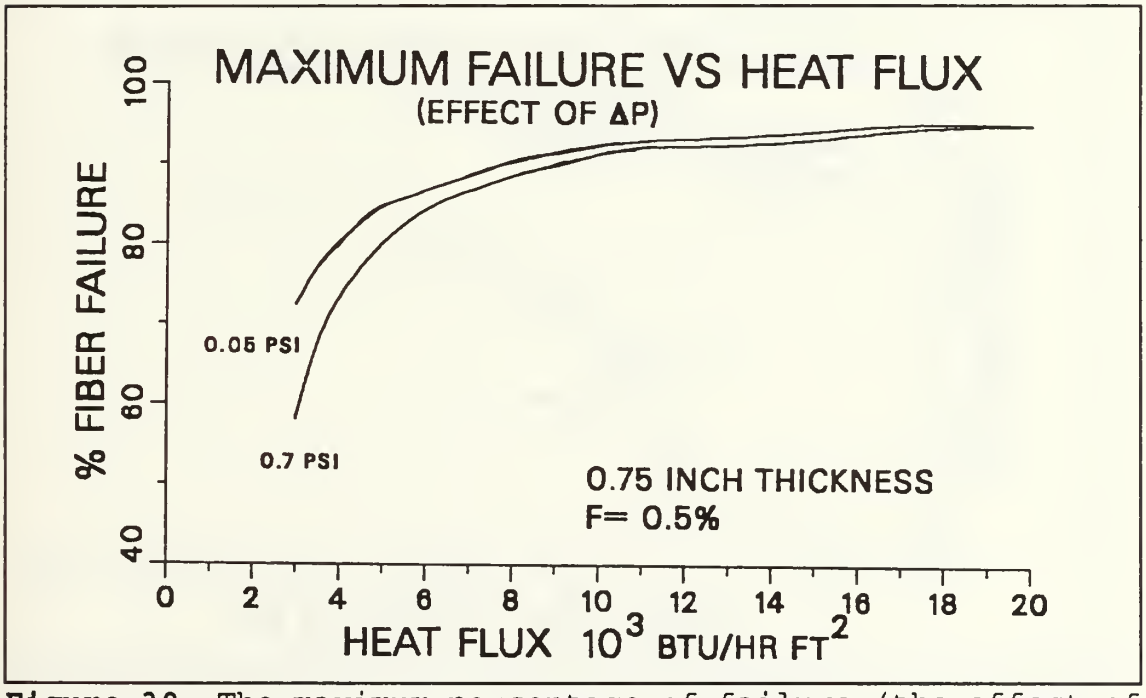

Figure 30: The maximum percentage of failure (the effect of ΔP) for 0.75", and F=0.5%.

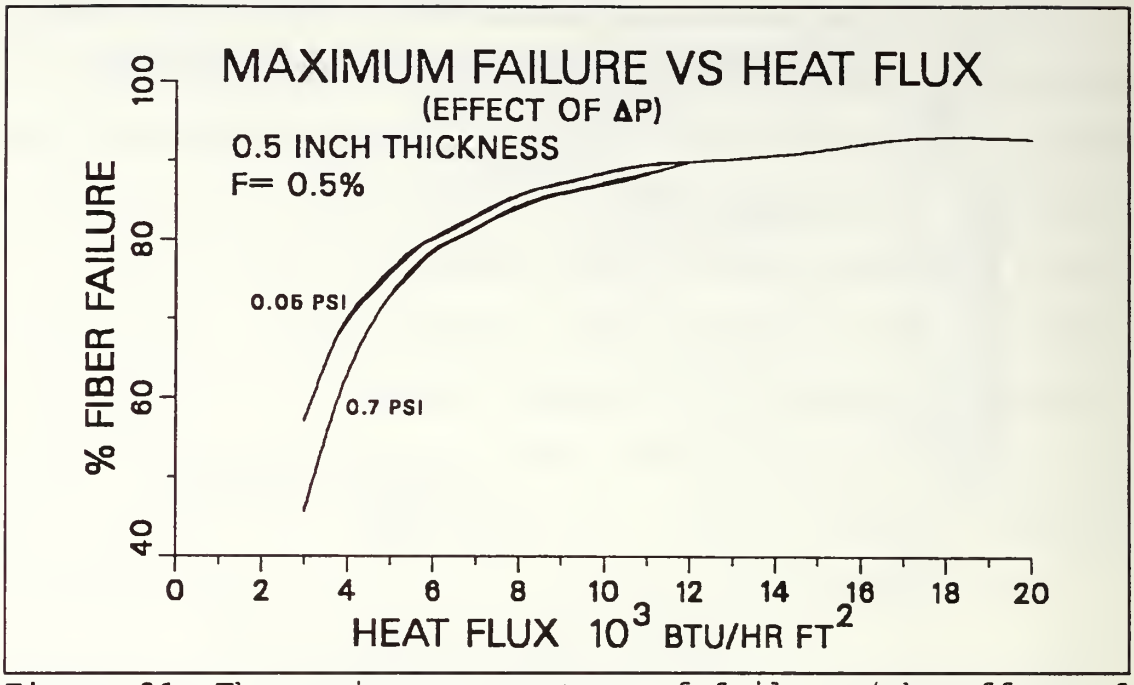

Figure 31: The maximum percentage of failure (the effect of ΔP) for 0.5", and F=0.5%.

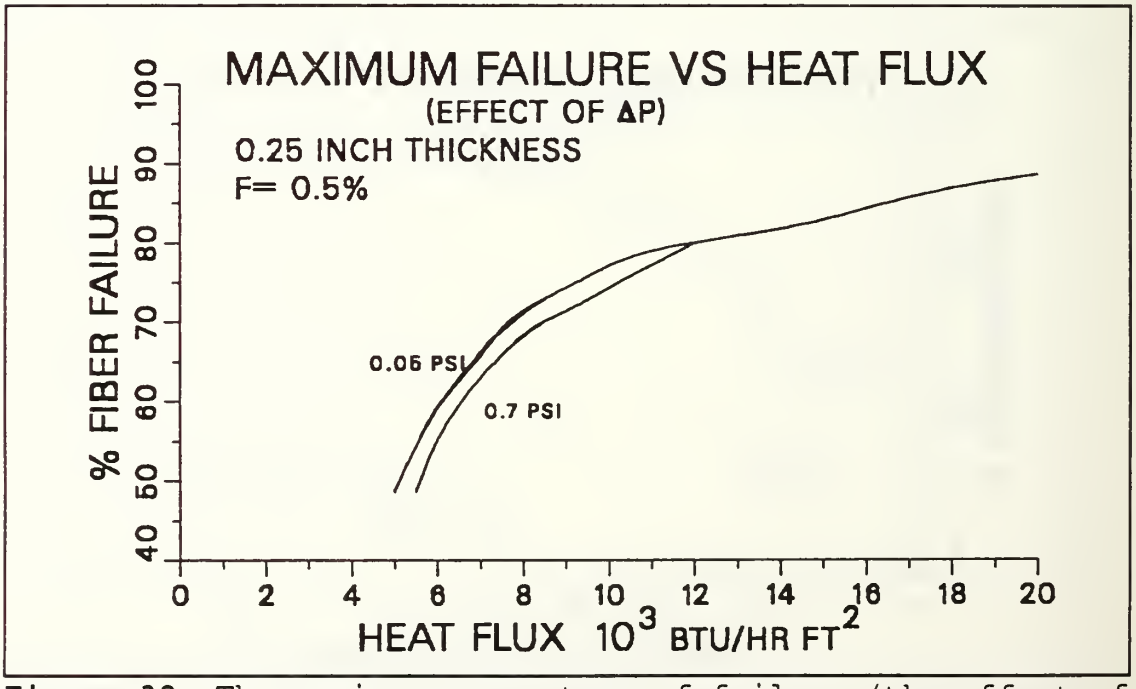

Figure 32: The maximum percentage of failure (the effect of ΔP) for 0.25", and F=0.5%.

G. MAXIMUM FAILURE (EFFECT OF F)

The effect of the combustion product fraction is shown in Figures 33 and 34. As expected, assuming a higher value of the combustion product fraction (F) reduces the amount of failure because of the increase in buckling strength. For the 0.25" plate there was no failure above a factor of 1.0% for range of heat fluxes investigated.

These trends were independent of differential pressure.

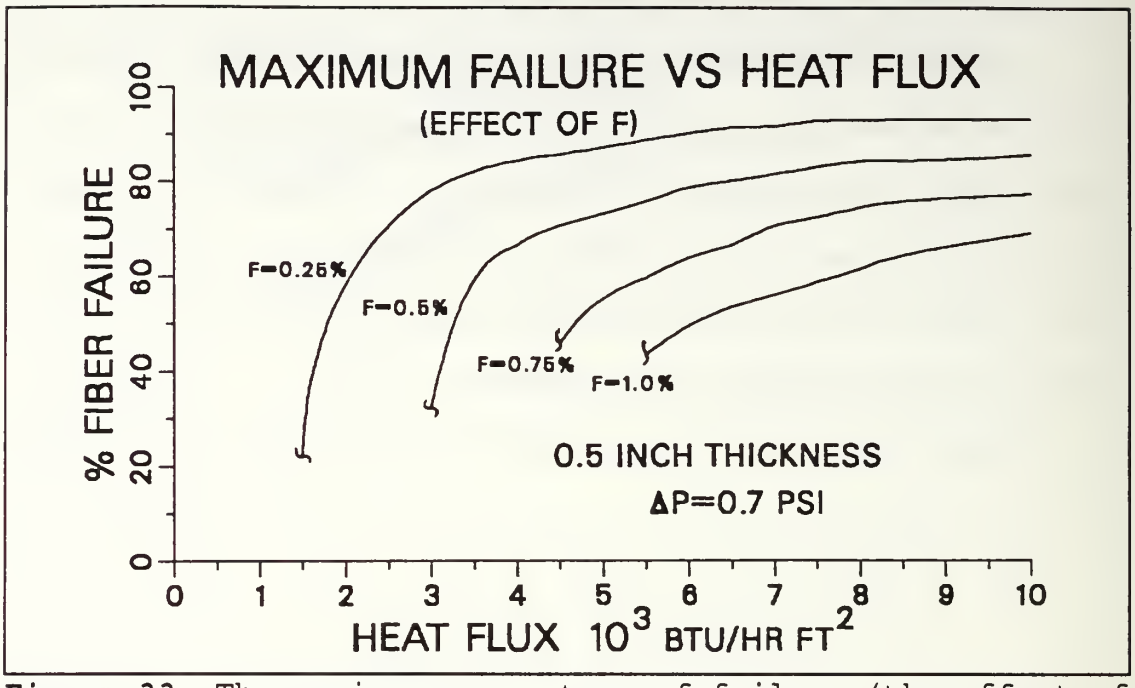

Figure 33: The maximum percentage of failure (the effect of combustion product fraction) 0.5", and ΔP=0.7 psi.

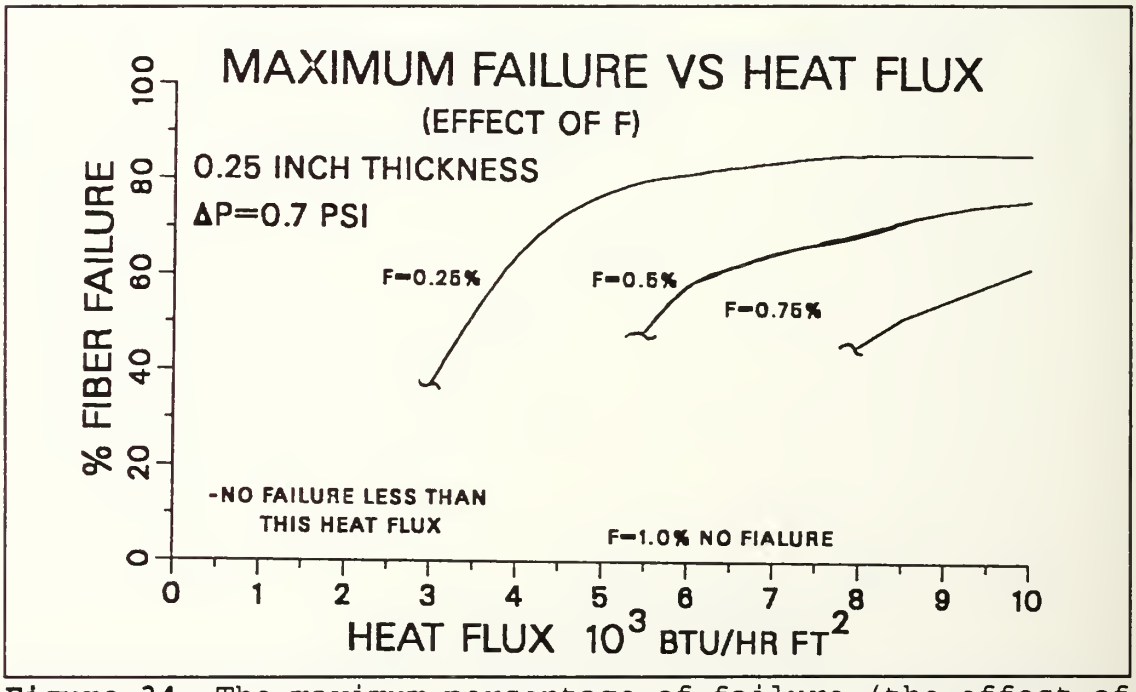

Figure 34: The maximum percentage of failure (the effect of combustion product fraction) 0.25" and ΔP=0.7.

H. MAXIMUM FAILURE (EFFECT OF THICKNESS)

As seen in Figures 35 and 36, the thickness of the material has minimal effect on the final percentage of material failure for higher heat fluxes. However at lower heat fluxes the thinner materials experience significantly less failure. In all cases the final percentage of fiber failure was between 42% and 97.5%.

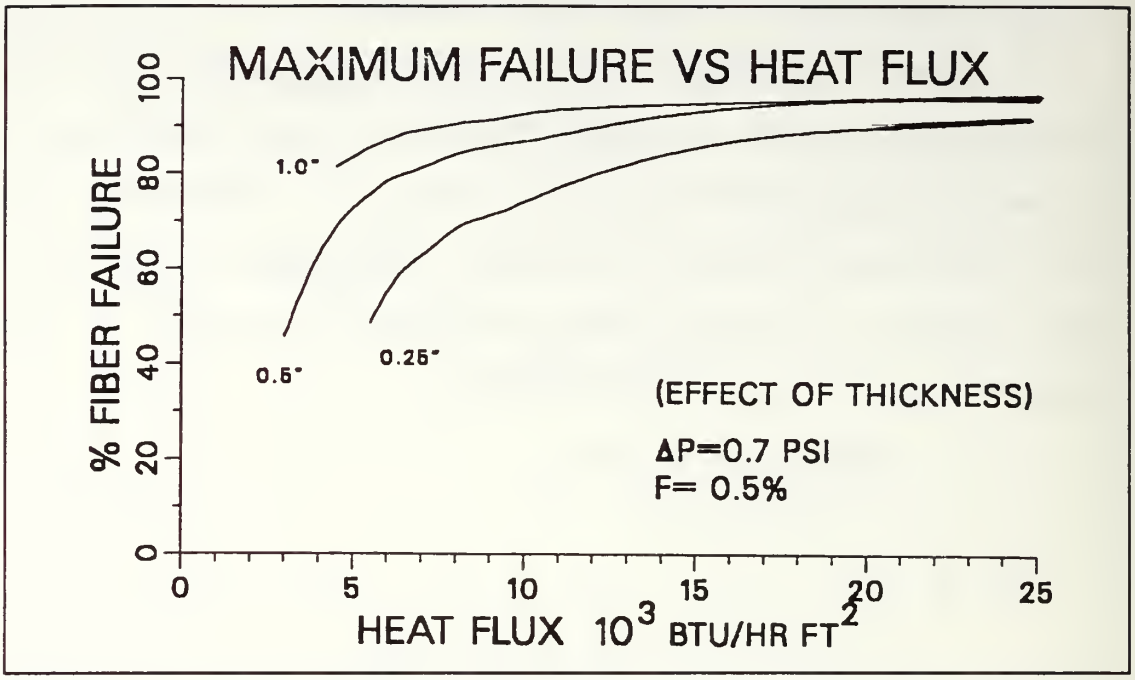

Figure 35: The maximum percentage of failure (the effect of material thickness) F=0.5%, ΔP=0.7 psi.

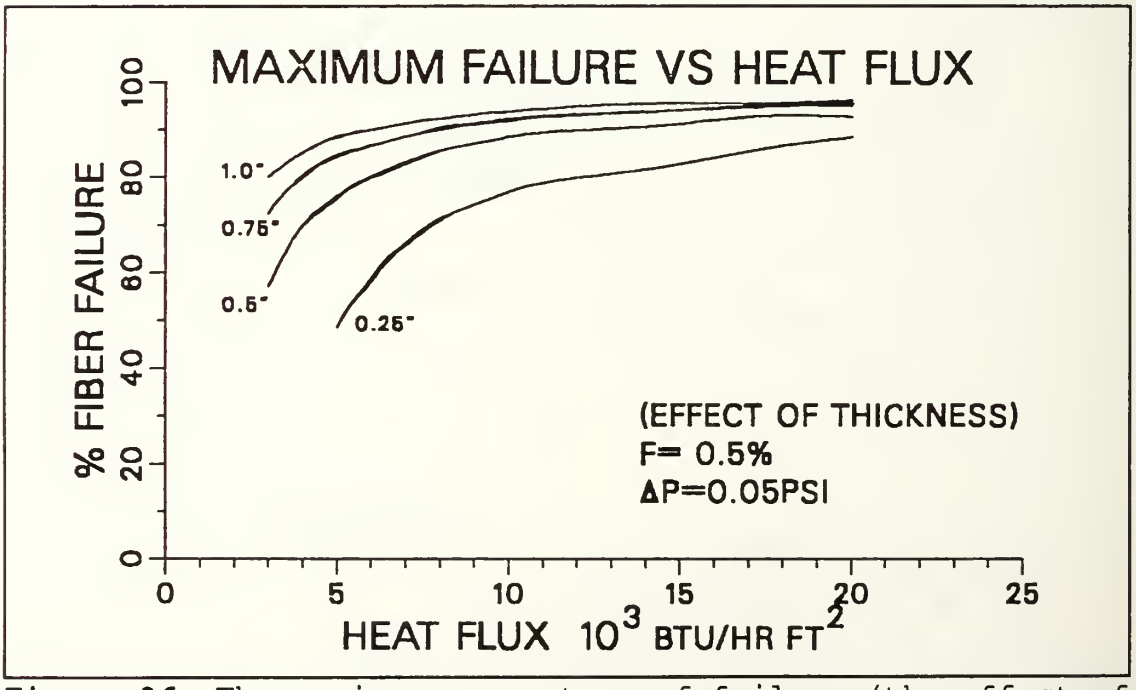

Figure 36: The maximum percentage of failure (the effect of material thickness) F=0.5%, and ΔP=0.05.

VI. CONCLUSIONS

The conclusions drawn from this study are as follows:

- The amount of time required before onset of fiber failure ranged from a very small 3 seconds (for a 0.25" plate at 25,000 btu/hr-ft^2) up to a maximum of 210 seconds (for a 1.0" plate at 2,000 btu/hr-ft^2). Given the reaction times of highly trained fire fighting teams onboard aircraft carriers, it is quite conceivable that failure may be averted for the longer onset of failure times.
- Once the failure of carbon graphite-epoxy composite material begins maximum failure occurs very quickly in less than 4 seconds. This time is of such short duration that reducing the amount of maximum failure once failure begins is not possible.
- The predominant factors effecting survivability of carbon-graphite epoxy composite materials are the heat flux applied, the combustion product factor and the thickness of the material. The differential pressure effect varies from very important at low heat fluxes to insignificant at high heat fluxes. However, the effect of differential pressure is mitigated by the fact that response times are in all cases very small at the high heat fluxes. Once failure occurs, maximum failures in the range of 80-90% preclude any future use of the material.

APPENDIX A: COMBUSTION CODE EQUATIONS

LIST OF EQUATION SYMBOLS

- μ - dynamic viscosity of air
- ϕ - oxygen concentration
- ρ_a - air density
- ρ_g - graphite density
- C_a - specific heat capacity of air
- C_g - specific heat capacity of graphite
- D_e - Mass diffusion coefficient
- h - convection heat transfer coefficient
- k_a - air thermal conductivity
- k_e - effective thermal conductivity of porus graphite
- k_r - pseudo thermal conductivity to account for radiation
- P - pressure
- p - porosity
- R_{O2} - oxygen reaction rate
- R_g - graphite reaction rate
- T_a - air temperature (^{o}R)
- T_g - graphite temperature (^{o}R)
- t - time
- u - pore velocity (of air)
- z - specific internal area

FINAL FIELD EQUATIONS

Following are the equations used in the Vatikiotis Combustion code. These equations are presented here in their form prior to non-dimensionalization. These equations were non-dimensionalized prior to use in the actual code.

THE GRAPHITE HEAT TRANSFER EQUATION

$$\frac{\partial}{\partial x}\left[(1-p)(k_e + k_r)\frac{\partial T_g}{\partial x}\right] - hz(T_g - T_a) + R_g z = (1-p)\rho_g C_g \frac{\partial T_g}{\partial t}$$

THE INTERNAL AIR HEAT TRANSFER EQUATION

$$\frac{\partial}{\partial x}\left(pk_a \frac{\partial T_a}{\partial x}\right) - p\rho_{a_a} C_a u \frac{\partial T_a}{\partial x} + hz(T_g - T_a) + u\frac{\partial (pP)}{\partial x} = \rho_a C_a \frac{\partial T_a}{\partial t}$$

OXYGEN TRANSPORT EQUATION

$$\frac{\partial}{\partial x}\left(pD_e \frac{\partial \phi}{\partial x}\right) - \frac{\partial}{\partial x}(p u \phi) - R_{O2} z = p\frac{\partial \phi}{\partial t}$$

THE INTERNAL FLOW EQUATION

$$\frac{d^2 P}{dx^2} + \left(\frac{1}{\rho_a}\frac{\partial \rho_a}{\partial x} + \frac{1}{m}\frac{\partial m}{\partial x} - \frac{1}{\mu}\frac{\partial \mu}{\partial x}\right)\frac{dP}{dx} - \frac{\mu}{\rho_a m}\frac{\partial (p\rho_a)}{\partial t} = 0$$

BOUNDARY CONDITIONS IMPOSED

For the X=0 location,

$$T_a = T_\infty$$

$$\phi = \phi_\infty$$

$$P = P_\infty$$

During heat addition $(1-p)(k_e + k_r)\frac{\partial T_g}{\partial x} = -q_{st}$

After fire is removed $(k_e + k_r)\frac{\partial T_g}{\partial x} = h_1(T_g - T_\infty) + \sigma\epsilon(T_g^4 - T_\infty^4)$

For the X=L location,

$$(k_e + k_r)\frac{\partial T_g}{\partial x} = h_1(T_g - T_\infty) - \sigma\epsilon(T_g^4 - T_\infty^4)$$

$$\frac{\partial T_a}{\partial x} = 0$$

$$\frac{\partial \phi}{\partial x} = 0$$

$$P = P_\infty + \Delta P$$

where:

q_{st} = the heat flux applied

T_∞ = ambient temperature (^oR)

ϕ_∞ = ambient oxygen concentration

h_1 and h_2 = convection heat transfer coefficients

INITIAL CONDITIONS

There are a number of ways to start these "combustion" problems. One way is to set the oxygen concentrations and the air and graphite temperatures to ambient conditions then apply an external heat source. This "natural" starting scheme requires some amount of computer effort to bring the plate up to conditions where temperatures have increased significantly. Instead of starting the problem at ambient conditions, computational effort can be reduced by starting the problem with the plate at elevated temperatures.

In this particular study the initial conditions were;

Graphite temperature $400^{o}F$

Air temperature $400^{o}F$

Oxygen concentration $0.0172\ lb/ft^{3}$ (ambient level).

APPENDIX B: STRESS ANALYSIS CODE

```
*EDWARD FAXLANGER JULY 1992
**********************************************************************
* THIS PROGRAM CALCULATES STRESSES INDUCED IN LONGITUDINAL FIBERS
* RESULTING FROM TEMPERATURE VARIATION ACROSS THE MEDIUM
**********************************************************************
C DESCRIPTION OF VARIABLES
C     U = DISPLACEMENTS OF NODAL POINTS
C    BC = VALUE OF THE TYPE I BOUNDARY CONDITION FOR NODAL POINT IBC
C     A = MATRIX CONTAINING INDIVIDUAL STIFFNESS
C     B = MATRIX CONTAINING INDIVIDUAL FORCE VECTOR
C    AA = MATRIX CONTAINING GLOBAL STIFFNESS
C    BB = MATRIX CONTAINING GLOBAL FORCE VECTOR
C     Y = LOCATIONS OF THE INDIVIDUAL FIBER (FROM BOTTOM OF PLATE)
C  TEMP = INTERPOLATED TEMPERATURE OF THE FIBER
C  DIAM = INTERPOLATED DIAMETER OF THE FIBER
C SIGMA = CALCULATED STRESS OF THE INDIVIDUAL FIBER
C   YIN = LOCATIONS OF NODAL POINTS FROM THE COMBUSTION CODE
C TEMPIN=TEMPERATURES FROM THE COMBUSTION CODE
C DIAMIN=THE DIAMETER AT THE NODAL POINT FROM THE COMBUSTION CODE
C   IBC = THE NUMBER OF THE NODE HAVING A TYPE I BOUNDARY CONDITION
C  NODES= A MATRIX USED FOR ELEMENT CONNECTIVITY TO THEIR NODAL POINTS
C    Y1 = LOCATION OF THE NODAL POINTS BROUGHT IN FROM VATIKIOTIS CODE
C NFLAG = A FLAG TO INDICATE TYPE OF FAILURE
C NELEM =A MATRIX CONTAINING THE NAMES OF THE UNBROKEN FIBERS
C    NE = NUMBER OF FIBER ELEMENTS
C NNODE = TOTAL NUMBER OF FIBER NODES
C PERCNT= PERCENTAGE OF ORIGINAL BUCKLING STRENGTH USED
C TSTREN= TENSILE STRENGTH OF FIBERS
C CSTREN= COMPRESSIVE STRENGTH OF FIBERS (NO BUCKLING)
C  EFIB = ELASTIC MODULUS OF THE FIBERS
C    VF = FIBER VOLUME FRACTION (ASSUMED CONSTANT)
C  EMAT = ELASTIC MODULUS OF THE MATRIX
C POISM = POISON RATIO OF THE MATRIX
C ALPHA = THERMAL EXPANSION COEFFICIENT (AXIAL)
C WIDTH = THE ASSUMED LENGTH OF EACH FIBER (ASSUMED TO BE ONE)
C TEMREF= REFERENCE TEMPERATURE (WHERE STRAIN EQUAL ZERO)
C   NNP = THE NUMBER OF NODAL POINTS READ IN FROM COMBUSTION CODE
C  TIME = TIME OF THE TEMPERATURE PROFILE BEING ANALYZED
C THICK = THE ORIGINAL THICKNESS OF THE MATERIAL (BEFORE BURNING)
C HEIGHT= THE THICKNESS OF THE MATERIAL AT THE PRESENT TIME
C NEUSED= THE NUMBER OF UNBROKEN FIBERS AT PRESENT TIME
C NELEM = A STORAGE OF UNBROKEN FIBERS NAMES
C  GMAT = SHEAR MODULUS OF THE EPOXY MATRIX MATERIAL
C
C MAIN PROGRAM
      IMPLICIT REAL*8(A-H,O-Z)
C THE FOLLOWING PARAMETER N1 SETS THE DIMENSION OF ARRAYS AND
C NEEDS TO BE EQUAL TO THE HIGHER OF 1)THE NUMBER OF NODES BEING
C READ IN **OR** 2) THE NUMBER OF ELEMENTS BEING ANALYZED
      PARAMETER (N1=101)
      PARAMETER (NN=2*N1)
C COMMON STATEMENT FOR MATERIAL PROPERTIES
```

```
COMMON/PROPER/TSTREN,CSTREN,EFIB,EMAT,ALPHA,WIDTH,THICK,POISM,VF
C
      REAL*8 U(NN),BC(NN),A(2,2),B(2),BB(NN),AA(NN,NN),Y(N1),
     &TEMP(N1),DIAM(N1),SIGMA(N1),YIN(N1),TEMPIN(N1),DIAMIN(N1)
      DIMENSION IBC(NN),NODES(NN,NN),INDEX(2),NFLAG(N1),NELEM(N1)

*THE FOLLOWING 3 STATEMENTS INCREASE THE NUMBER OF EQUATIONS
*THAT THE EQUATION SOLVER DLSARG WILL HANDLE. IF LARGER SPACE IS
* NEEDED DLSARG WILL GIVE AN ERROR MESSAGE AND RECOMMEND LARGER
* WORK SPACES
      COMMON/WORKSP/RWKSP
      REAL RWKSP(82236)
      CALL IWKIN(82236)
C DATA FILE FOR OUTPUT OF DATA
      OPEN(UNIT=11, FILE='/TEST31 STRESS B1',STATUS='OLD')
C DATA FILE FOR READING INPUT DATA
      OPEN(UNIT=12, FILE='/TEST31 TEMPER B1',STATUS='OLD')
C NE IS THE NUMBER OF FIBERS ASSUMED FOR ANALYSIS
      NE=30
      NNODE=NE*2
C ENTER THE PERCENTAGE OF MATRIX SUPPORT
      PERCNT=.005

C FIBER CHARACTERISTICS; LONGITUDINAL COMPRESSIVE AND TENSILE
C STRENGTHS (PSI), ELASTIC MODULUS AND THERMAL COEFFICIENT
      TSTREN=300.0D3
      CSTREN=-260.0D3
      EFIB=31.0D6
      EMAT=.5D6
      VF=.196
      POISM=.35
      ALPHA=-0.55D-6
C WIDTH OF SIMULATED HOLE (LENGTH OF FIBERS) ASSUMED TO BE UNITY
C SINCE IT HAS NO EFFECT ON PROBLEM
      WIDTH=1.0D0
C REFERENCE TEMPERATURE IN DEGREES F WHERE INITIAL STRESSES WERE ZERO
      TEMREF= 60.D0

C INITIALIZE FLAGS TO ZERO (NFLAG KEEPS TRACK OF BROKEN FIBERS)
C                          (NSTOP STOPS THE PROGRAM           )
      NSTOP=0
      DO M=1,NE
      NFLAG(M)=0
      END DO


* READ IN OF INFORMATION FROM COMBUSTION CODE OUTPUT
      READ(12,*)NNP
      CALL CHECK(NNP,NSTOP)
      IF(NSTOP.NE.0)GOTO 100
      CALL READER(N1,NNP,TIME,HEIGHT,YIN,TEMPIN,DIAMIN,NSTOP)
      IF(NSTOP.NE.0)GOTO 100

*LOOP FOR FILLING ALL ELEMENT HEIGHTS ASSUMING EVEN SPACING
      THICK=HEIGHT
      YINC=THICK/(NE)
      YSTART=YINC/2
      DO M=1,NE
      Y(M)=YSTART+YINC*(M-1)
      END DO
```

```
 200  BURN=THICK-HEIGHT
C INITIALIZE ARRAYS TO ZERO
      DO I=1,NN
      BB(I)=0.0D0
      DO J=1,NN
      AA(I,J)=0.0D0
      END DO
      END DO

      DO I=1,NE
C IF THE FIBERS ARE ALREADY CONSUMED BY COMBUSTION (OUTSIDE EDGE)
C NULL THEIR EFFECT BY SETTING THEIR FLAG TO 1
      IF(Y(I).LT.BURN)THEN
      NFLAG(I)=1
      END IF
C DETERMINE THE TEMPERATURE AND DIAMETER OF NON-FAILED FIBERS THIS
C LOOP IS FOR INTERPOLATION OF DATA RECEIVED FROM "STRESS INPUT" FILE.
C THE RECEIVED DATA IS IN RELATIVE SPACING AND MUST BE CHANGED TO
C ABSOLUTE SPACING IN ORDER TO DETERMINE PERCENTAGE FAILURE OF FIBERS
C INTERPOLATE NON-BROKEN FIBERS ONLY
      IF(NFLAG(I).EQ.0) THEN
      DO N=1,NNP-2
      IF((Y(I).GE.YIN(N)+BURN).AND.(Y(I).LE.YIN(N+2)+BURN))THEN
      CALL INTERP(YIN(N)+BURN,YIN(N+1)+BURN,YIN(N+2)+BURN,
     &DIAMIN(N),DIAMIN(N+1),DIAMIN(N+2),Y(I),DIAM(I))
      CALL INTERP(YIN(N)+BURN,YIN(N+1)+BURN,YIN(N+2)+BURN,
     &TEMPIN(N),TEMPIN(N+1),TEMPIN(N+2),Y(I),TEMP(I))
      END IF
      END DO
      END IF
      END DO

C LOOP FOR DETERMINING THE ELEMENTS THAT ARE NOT BROKEN (IE THE
C ONES THAT ARE TO BE ANALIZED)
      NEUSED=0
      DO I=1,NE
      IF(NFLAG(I).EQ.0) THEN
      NEUSED=NEUSED+1
      NELEM(NEUSED)=I
      END IF
      END DO
      IF(NEUSED.LT.2)THEN
      WRITE(11,*)'ALL BUT TWO ELEMENTS HAVE BROKEN'
      WRITE(11,*)'ANALYSIS IS STOPPED/PROGRAM STOPPED'
      GOTO 100
      END IF
      NNUSED=NEUSED*2

* LOOP FOR ESTABLISHING CONNECTIVITY OF NODES TO THEIR ELEMENTS
* FOR USE IN BUILDING GLOBAL MATRIX AND GLOBAL VECTOR
      L=1
      DO I=1,NEUSED
      DO J=1,2
      NODES(I,J)=L
      L=L+1
      END DO
      END DO


* LOOP TO BUILD GLOBAL MATRIX(AA) AND VECTOR(BB)
      DO IE=1,NEUSED
```

```
      CALL MATRIX(A,B,TEMP(NELEM(IE))-TEMREF,DIAM(NELEM(IE)))
      INDEX(1)=NODES(IE,1)
      INDEX(2)=NODES(IE,2)
      DO I=1,2
      II=INDEX(I)
      BB(II)=BB(II)+B(I)
      DO J=1,2
      JJ=INDEX(J)
      AA(II,JJ)=AA(II,JJ)+A(I,J)
      END DO
      END DO
      END DO

*LOOP FOR TYPE I BOUNDARY CONDITION INITIALIZATION
      DO I=1,NNUSED-1,2
      IBC(I)=I
      BC(I)=0.0D0
      END DO

* APPLY TYPE 1 BOUNDARY CONDITIONS
      DO I=1,NNUSED-1,2
      J=IBC(I)
      DO K=1,NNUSED
      BB(K)=BB(K)-BC(I)*AA(K,J)
      AA(K,J)=0.0
      AA(J,K)=0.0
      AA(J,J)=1.0
      BB(J)=BC(I)
      END DO
      END DO

C APPLY TYPE 2 BOUNDARY CONDITIONS
      DO J=2,NNUSED-2,2
      CALL MOD2FL(NN,NNUSED,J,J+2,-1.0D0,0.0D0,AA,BB)
      END DO

C SOLVE THE SYSTEM OF EQUATIONS USING IMSL LIBRARY
      CALL DLSARG(NNUSED,AA,NN,BB,1,U)

      DO I=1,NE
      SIGMA(I)=0.0D0
      END DO
      DO I=1,NEUSED
      STRAIN=U(I*2)/WIDTH
      SIGMA(NELEM(I))=EFIB*(STRAIN-ALPHA*(TEMP(NELEM(I))-TEMREF))
      END DO

C LOOP TO CALCULATE STRESSES OF EACH ELEMENT AND OUTPUT RESULTS
C TO OUTPUT FILE
      WRITE(11,9)TIME
      WRITE(11,6)
      DO I=1,NE
      IF(NFLAG(I).NE.0)WRITE(11,8) I,NFLAG(I)
      IF(NFLAG(I).EQ.0)WRITE(11,7)I,SIGMA(I),DIAM(I)
      END DO
  6   FORMAT(5X,'FIBER NUMBER',5X,'FIBER STRESS (PSI)',2X,'DIAMETER')
  7   FORMAT(12X,I3,11X,G10.4,6X,G10.4,3X,G11.4,2X,I1)
  8   FORMAT(17X,I3,4X,'PREVIOUSLY BROKEN,  NFLAG=',I1)
  9   FORMAT(1X,'TIME=',F8.3,' SECONDS')
      CALL BROKEN(N1,NE,SIGMA,DIAM,NFLAG,BROKE,PERCNT)
      WRITE(11,*)'****************************************'
```

```
      WRITE(11,*)
      CALL READER(N1,NNP,TIME,HEIGHT,YIN,TEMPIN,DIAMIN,NSTOP)
      IF(NSTOP.NE.0)GOTO 100
      GOTO 200
 100  END
C
C
      SUBROUTINE MATRIX(A,B,TEMP,DIAM)
C THIS SUBROUTINE CALCULATES THE ELEMENT LEVEL
C STIFFNESS MATRIX(A) AND VECTOR(B)
      IMPLICIT REAL*8(A-H,O-Z)
      COMMON/PROPER/TSTREN,CSTREN,EFIB,EMAT,ALPHA,WIDTH,THICK,POISM,VF
      REAL*8 A(2,2),B(2)
      PI=4*ATAN(1.0)
      AREA=DIAM*DIAM*PI/4.0
      S=AREA*EFIB/WIDTH
      A(1,1)=S
      A(1,2)=-S
      A(2,1)=-S
      A(2,2)=S
      B(2)=EFIB*AREA*ALPHA*TEMP
      B(1)=-B(2)
      END
C
C
      SUBROUTINE BROKEN(N1,NE,STRESS,DIAM,NFLAG,BROKE,PERCNT)
C THIS SUBROUTINE DETERMINES THE NUMBER OF BROKEN FIBERS (BROKE)
C DUE TO TENSILE AND COMPOSITE BUCKLING
C NFLAG EQUALS 0:FOR UNFAILED FIBER
C              1:FOR BURNT AWAY FIBERS
C              2:FOR OVER STRESS BY TENSION
C              3:FOR OVER STRESS BY BUCKLING
      IMPLICIT REAL*8(A-H,O-Z)
      COMMON/PROPER/TSTREN,CSTREN,EFIB,EMAT,ALPHA,WIDTH,THICK,POISM,VF
      REAL*8 STRESS(N1),DIAM(N1)
      DIMENSION NFLAG(N1)
      PI=4*ATAN(1.0)
C CALCULATE COMPOSITE BUCKLING STRENGTH OF THE FIBER
C AS A FRACTION OF THE ORIGINAL COMPOSITE BUCKLING STRENGTH
        GMAT=EMAT/(2.*(1.+POISM))
        BUCKLE=-GMAT/(1.-VF)*PERCNT
      DO I=1,NE
C DO NOT CHECK PREVIOUSLY BROKEN FIBERS
      IF(NFLAG(I).EQ.0) THEN
C CHECK FOR TENSILE STRESS FAILURE
        IF(STRESS(I).GE.TSTREN) THEN
          NFLAG(I)=2
        END IF
C CHECK FOR BUCKLING FAILURE
        IF(STRESS(I).LE.BUCKLE) THEN
          NFLAG(I)=3
        END IF
      END IF
      END DO
C SUMMATION OF EACH TYPE OF BREAKAGE
      BURNT=0.0
      TENSIL=0.0
      BUCK=0.0
      DO I=1,NE
      IF(NFLAG(I).EQ.1)  BURNT=BURNT+1
      IF(NFLAG(I).EQ.2)  TENSIL=TENSIL+1
```

```
      IF(NFLAG(I).EQ.3)  BUCK=BUCK+1
      END DO
      TBROKE=BURNT+TENSIL+BUCK
      WRITE(11,5)BURNT*100/NE
    5 FORMAT(1X,'PERCENTAGE BURNT FIBERS',F5.1)
      WRITE(11,4)TENSIL*100/NE
    4 FORMAT(1X,'PERCENTAGE BROKEN IN TENSILE MODE',F5.1)
      WRITE(11,2)BUCK*100/NE
    2 FORMAT(1X,'PERCENTAGE OF BUCKLED FIBERS',F5.1)
      WRITE(11,1)TBROKE*100/NE
    1 FORMAT(1X,'TOTAL PERCENTAGE OF FAILED FIBERS',F5.1)
      END
C
C
      SUBROUTINE INTERP(X1,X2,X3,Y1,Y2,Y3,XX,YY)
C THIS SUBROUTINE TAKES 3 X VALUES, 3 Y VALUES. THEN USING A GIVE XX
C VALUE PERFORMS QUADRATIC INTERPOLATION TO DETERMINE THE YY VALUE.
      IMPLICIT REAL*8(A-H,O-Z)
      REAL*8 A(3,3),B(3),C(3)
      A(1,1)=1.D0
      A(2,1)=1.D0
      A(3,1)=1.D0
      A(1,2)=X1
      A(2,2)=X2
      A(3,2)=X3
      A(1,3)=X1**2.
      A(2,3)=X2**2.
      A(3,3)=X3**2.
      B(1)=Y1
      B(2)=Y2
      B(3)=Y3
C
C CALLING IMSL LIBRARY SUBROUTINE TO SOLVE A(3,3)*C(3)=B(3)
C TO DETERMINE THE QUADRATIC COEFFICIENTS
      CALL DLSARG(3,A,3,B,1,C)
      YY=C(1)+C(2)*XX+C(3)*XX**2.
      END
C
      SUBROUTINE MOD2FL(NN,NSIZE,L1,L2,A,B,S,C)
      IMPLICIT REAL*8 (A-H,O-Z)
      DIMENSION  S(NN,NN), C(NN)
C     * * * * * * * * * * * * * * * * * * * * * * * * * * *
C     APPLY TYPE 2 CONSTRAINTS TO FULL EQUATIONS
C     METHOD AND SUBROUTINE BY: J. ED AKIN
C     * * * * * * * * * * * * * * * * * * * * * * * * * * *
C     NN = THE TOTAL SIZE OF THE PASSED
C     NSIZE = WORKING SIZE OF ARRAYS
C     S = FULL SQUARE MATRIX
C     C = COLUMN MATRIX
C     L1,L2 = CONSTRAINED DEGREES OF FREEDOM SUBCRIPTS OF D MATIRX
C     A,B = CONSTRAINT COEFFICIENTS
C        D(L1) + A*D(L2) = B  ,   S*D = C
C     INITIAL CALCULATIONS
      S12 = S(L1,L2)
      C11 = C(L1)
C     SUBTRACT A*COLUMN L1 FROM COLUMN L2
C     SUBTRACT B*COLUMN L1 FROM C
      DO 10  I = 1,NSIZE
      S(I,L2) = S(I,L2) - A*S(I,L1)
      S(L2,I) = S(I,L2)
      C(I) = C(I) - B*S(I,L1)
```

```
      S(I,L1) = 0.0
      S(L1,I) = 0.0
 10   CONTINUE
      S(L1,L1) = 1.0
      S(L2,L2) = S(L2,L2) - A*S12 + A*A
      S(L2,L1) = A
      S(L1,L2) = A
      C(L1) = B
      C(L2) = C(L2) - A*C11 + A*B
      RETURN
      END
C
C
      SUBROUTINE READER(N1,NNP,TIME,HEIGHT,YIN,TEMPIN,DIAMIN,NSTOP)
C THIS SUBROUTINE READS IN THE NODAL POINT VALUES FROM THE
C COMBUSTION CODE
      IMPLICIT REAL*8(A-H,O-Z)
      REAL*8 YIN(N1),TEMPIN(N1),DIAMIN(N1)
      READ(12,*,END=10)
      READ(12,*,END=10)
      READ(12,*,END=10)
      READ(12,*,END=10) TIME
      READ(12,*,END=10)
      READ(12,*,END=10) HEIGHT
      READ(12,*,END=10)
C CONVERT HEIGHT TO INCHES
      HEIGHT=HEIGHT*12.0
      DO I=1,NNP
      READ(12,*,END=10) K,YIN(I),TEMPIN(I),DIAMIN(I)
C CONVERT INPUT LOCATION(YIN) AND DIAMETER(DIAMIN) TO INCHES
      YIN(I)=YIN(I)*12.0
      DIAMIN(I)=DIAMIN(I)*12.0
      END DO
      GOTO 20
  10  NSTOP=1
  20  END
C
C
      SUBROUTINE CHECK(NNP,NSTOP)
C QUICK CHECK TO SEE IF THE NUMBER OF INPUT NODAL POINTS IS ODD
C SO QUADRATIC INTERPOLATION CAN BE USED.  IF NOT STOP PROGRAM
      MCHECK=MOD(NNP,2)
      IF(MCHECK.EQ.0) THEN
      WRITE(*,2)'THE NUMBER OF INPUT NODAL POINTS MUST BE AN ODD'
      WRITE(*,2)'NUMBER IN ORDER FOR THIS PROGRAM TO USE QUADRATIC'
      WRITE(*,2)'INTERPOLATION. CHECK NNP IN INPUT DATA'
      WRITE(*,2)'THIS PROGRAM IS STOPPED'
  2   FORMAT(1X,A)
      NSTOP=1
      END IF
      END
```

APPENDIX C: SAMPLE OUTPUT DATA FROM STRESS CODE

TIME= 0.000 SECONDS

FIBER NUMBER	FIBER STRESS (PSI)	DIAMETER
1	0.0000E+00	0.8333E-02
2	0.0000E+00	0.8333E-02
3	0.0000E+00	0.8333E-02
4	0.0000E+00	0.8333E-02
5	0.0000E+00	0.8333E-02
6	0.0000E+00	0.8333E-02
7	0.0000E+00	0.8333E-02
8	0.0000E+00	0.8333E-02
9	0.0000E+00	0.8333E-02
10	0.0000E+00	0.8333E-02
11	0.0000E+00	0.8333E-02
12	0.0000E+00	0.8333E-02
13	0.0000E+00	0.8333E-02
14	0.0000E+00	0.8333E-02
15	0.0000E+00	0.8333E-02
16	0.0000E+00	0.8333E-02
17	0.0000E+00	0.8333E-02
18	0.0000E+00	0.8333E-02
19	0.0000E+00	0.8333E-02
20	0.0000E+00	0.8333E-02
21	0.0000E+00	0.8333E-02
22	0.0000E+00	0.8333E-02
23	0.0000E+00	0.8333E-02
24	0.0000E+00	0.8333E-02
25	0.0000E+00	0.8333E-02
26	0.0000E+00	0.8333E-02
27	0.0000E+00	0.8333E-02
28	0.0000E+00	0.8333E-02
29	0.0000E+00	0.8333E-02
30	0.0000E+00	0.8333E-02

PERCENTAGE BURNT FIBERS 0.0
PERCENTAGE BROKEN IN TENSILE MODE 0.0
PERCENTAGE OF BUCKLED FIBERS 0.0
TOTAL PERCENTAGE OF FAILED FIBERS 0.0
****

TIME= 8.810 SECONDS

FIBER NUMBER	FIBER STRESS (PSI)	DIAMETER
1	2777.	0.8333E-02
2	2236.	0.8333E-02
3	1791.	0.8333E-02
4	1385.	0.8333E-02
5	1022.	0.8333E-02
6	705.4	0.8333E-02
7	433.8	0.8333E-02
8	206.0	0.8333E-02
9	18.97	0.8333E-02
10	-131.2	0.8333E-02
11	-249.3	0.8333E-02
12	-340.1	0.8333E-02
13	-408.6	0.8333E-02
14	-459.2	0.8333E-02
15	-495.9	0.8333E-02
16	-522.0	0.8333E-02
17	-540.2	0.8333E-02
18	-552.6	0.8333E-02
19	-561.0	0.8333E-02
20	-566.6	0.8333E-02
21	-570.3	0.8333E-02
22	-572.6	0.8333E-02
23	-574.1	0.8333E-02
24	-575.1	0.8333E-02
25	-575.7	0.8333E-02
26	-576.0	0.8333E-02
27	-576.3	0.8333E-02
28	-576.4	0.8333E-02
29	-576.5	0.8333E-02
30	-576.5	0.8333E-02

PERCENTAGE BURNT FIBERS 0.0
PERCENTAGE BROKEN IN TENSILE MODE 0.0
PERCENTAGE OF BUCKLED FIBERS 0.0
TOTAL PERCENTAGE OF FAILED FIBERS 0.0
****

TIME= 17.810 SECONDS

FIBER NUMBER	FIBER STRESS (PSI)	DIAMETER
1	3524.	0.8333E-02
2	3022.	0.8333E-02
3	2597.	0.8333E-02
4	2190.	0.8333E-02
5	1805.	0.8333E-02
6	1443.	0.8333E-02
7	1107.	0.8333E-02
8	797.8	0.8333E-02
9	515.9	0.8333E-02
10	261.7	0.8333E-02
11	34.97	0.8333E-02
12	-165.1	0.8333E-02
13	-339.8	0.8333E-02
14	-490.6	0.8333E-02
15	-619.4	0.8333E-02
16	-728.2	0.8333E-02
17	-819.1	0.8333E-02
18	-894.3	0.8333E-02
19	-955.8	0.8333E-02
20	-1006.	0.8333E-02
21	-1046.	0.8333E-02
22	-1077.	0.8333E-02
23	-1102.	0.8333E-02
24	-1122.	0.8333E-02
25	-1136.	0.8333E-02
26	-1148.	0.8333E-02
27	-1156.	0.8333E-02
28	-1161.	0.8333E-02
29	-1165.	0.8333E-02
30	-1167.	0.8333E-02

PERCENTAGE BURNT FIBERS 0.0
PERCENTAGE BROKEN IN TENSILE MODE 0.0
PERCENTAGE OF BUCKLED FIBERS 13.3
TOTAL PERCENTAGE OF FAILED FIBERS 13.3
****

```
TIME=  26.560 SECONDS
    FIBER NUMBER     FIBER STRESS (PSI)  DIAMETER
              1             1389.          0.8333E-02
              2             1519.          0.8333E-02
              3             1520.          0.8333E-02
              4             1392.          0.8333E-02
              5             1174.          0.8333E-02
              6             902.0          0.8333E-02
              7             603.2          0.8333E-02
              8             297.3          0.8333E-02
              9            -3.231          0.8333E-02
             10            -290.8          0.8333E-02
             11            -561.4          0.8333E-02
             12            -812.8          0.8333E-02
             13            -1044.          0.8333E-02
             14            -1255.          0.8333E-02
             15            -1445.          0.8333E-02
             16            -1616.          0.8333E-02
             17            -1768.          0.8333E-02
                  18    PREVIOUSLY BROKEN,  NFLAG=3
                  19    PREVIOUSLY BROKEN,  NFLAG=3
                  20    PREVIOUSLY BROKEN,  NFLAG=3
                  21    PREVIOUSLY BROKEN,  NFLAG=3
                  22    PREVIOUSLY BROKEN,  NFLAG=3
                  23    PREVIOUSLY BROKEN,  NFLAG=3
                  24    PREVIOUSLY BROKEN,  NFLAG=3
                  25    PREVIOUSLY BROKEN,  NFLAG=3
                  26    PREVIOUSLY BROKEN,  NFLAG=3
                  27    PREVIOUSLY BROKEN,  NFLAG=3
                  28    PREVIOUSLY BROKEN,  NFLAG=3
                  29    PREVIOUSLY BROKEN,  NFLAG=3
                  30    PREVIOUSLY BROKEN,  NFLAG=3
PERCENTAGE BURNT FIBERS  0.0
PERCENTAGE BROKEN IN TENSILE MODE  0.0
PERCENTAGE OF BUCKLED FIBERS 56.7
TOTAL PERCENTAGE OF FAILED FIBERS 56.7
****************************************
```

APPENDIX D: SAMPLE INPUT DATA TO COMBUSTION CODE

```
 80.E0      TAMB     AMBIENT TEMPERATURE
  50.4E0    UINF     DIFF. PRESS. ACROSS MEDIUM LB/FT2 OR SURF VELOCITY
 2116.8E0   PAMB     AMBIENT PRESSURE LB/FT2
   1.4E0    TORT     TORTUOSITY OF THE MEDIUM
0.868055555555555507E-03  DINT      LUMP FIBER DIAMETER PER CELL
0.868055555555555507E-03  SINIT     DISTANCE BETWEEN LUMPED FIBERS
0.416666666666666667E-01  XLENGTH   TOTAL MEDIUM THICKNESS
0.416666666666666667E-01  XINIT     INITIAL THICKNESS OF THE MEDIUM
 53.34E0    RGAS      THE GAS CONSTANT FOR AIR
 86.0E0     GCOND     THERMAL CONDUCTIVITY OF GRAPHITE
 0.231E0    SPHTG     SPECIFIC HEAT OF GRAPHITE
 70.3E0     ROG       DENSITY OF GRAPHITE
 0.9E0      EMIS      THE EMISSIVITY OF THE GRAPHITE
 .91E0      PHI       SHAPE FACTOR 1.0 FOR SPHERE .91 FOR CYLINDERS
 1.0E0      HLENTH    REF LENGTH FOR SURFACE HEAT TRANSFER (NORMALLY 1)
 14085.E0   ENTHAL    THE ENTHALPY OF CHEMICAL REACTION
 0.5E0      ORDNTH    THE ORDER OF THE CHEMICAL REACTION
 0.5E0      EXTEMP    THE EXPONENT OF THE TEMPERATURE FOR REACTION RATE
 0.375E0    STIOCH    STOICHIOMETRIC RATIO FOR THE REACTION
 2.065E6    RECOEFF   ARRHENIUS EQUATION COEFFICIENT
 28836.E0   ENERGY    ACTIVATION ENERGY DIVIDED BY THE IDEAL GAS CONSTANT
 30000.E0   SQ        THE HEAT FLUX (SIMULATING THE FIRE)
  4.D0      T         THE APPROXIMATE TIME INTERVAL FOR PRINTING RESULTS
  0.E0      TSTART    THE STARTING TIME OF THE PROBLEM
 200.E0     TSTOP     THE STOP TIME OF THE PROBLEM
 40.E0      TQ        THE HEATER TURN OFF TIME (FIRE IS OUT)
 1.00D-5    HSTART    THE INITIAL TIME INTERVAL IN SUBROUTINE SDESOL
 1.E-10     HMIN      THE MINIMUM TIME INTERVAL FOR SUBROUTINE SDESOL
 0.500      HMAX      THE MAXIMUM TIME INTERVAL FOR SUBROUTINE SDESOL
 0.0010     RMSEPS    ERROR CRITERIA FOR SUBROUTINE SDESOL
 2500.E0    TMAX      THE MAX TEMP ON PRINTER PLOTS (Y AXIS)
 50.E0      TMIN      THE MIN TEMP ON PRINTER PLOTS (Y AXIS)
 .020E0     CMAX      THE MAX OXYGEN CONC. ON PRINTER PLOTS (Y AXIS)
 -.001E0    CMIN      THE MIN OXYGEN CONC. ON PRINTER PLOTS (YAXIS)
 0.E0       SL1       SLOPE FOR A LINEAR PROFILE FOR GRAPHITE TEMP
 0.E0       SL2       SLOPE FOR A LINEAR PROFILE FOR AIR TEMP
 0.E0       SL3       SLOPE FOR A LINEAR PROFILE FOR CONCENTRATION
  6  MAXDER  MAX ORDER EQUATION SOLVER USED IN SDESOL
  0  IPRT    PRINT PARAMETER FOR SDESOL
  1  ITIME   MULTIPLIER OF PRINT TIME STEP ONCE PROGRAM IS IN SURF RECESS
  25 NNP     NUMBER OF NODAL POINTS
  0  IELEM   0=AUTO 1=USER INPUT(SEE BELOW) OF NODAL LOCATIONS
  0  IDIAM   0=AUTO 1=USER INPUT(SEE BELOW) OF PARTICLE DIAMETER
  0  ISPACE
  0  IUNIF   0=UINF IS DIFFERENTIAL PRESSURE 1=UNIF IS SURFACE VELOCITY
  0  IREAC   0=AUTO STOICH. RATIO OF CARBON OXIDES 1=USER ENTRY OF RATIO
  12 IBC     BOUNDARY CONDITION PARAMETER
  1  IIC     1=AUTO LINEAR TEMPG, TEMPA, CONC. O2 0=USER ENTRY(SEE BELOW)
  0  IQ      LOCATION OF HEATER 0=HEATER AT ZERO 1=HEATER AT XLENGTH
  500 NSTOP  MAX NUMBER OF TIMES ALLOWED THROUGH INTEGRATION LOOPS
  0   ITRIP  LEAVE ZERO UNLESS RESTARTING PROGRAM IN SURF RECESSION MODE
800.E0   --GRAPHITE TEMP NODE 1]*THESE 3 ITEMS ARE REQUIRED ONLY
```

```
800.E0    - AIR TEMP NODE 1-----]*IF IIC=1. THEY MUST FOLLOW "ITRIP" OR
.0172E0   --OXYGEN CONC NODE 1--]*MANUAL ENTRY OF NODE LOCATIONS IF USED
  0.D0 ******THE FOLLOWING DATA IS THE X LOCATION OF THE NODES
.001D0      *THESE LOCATIONS ARE ONLY NEEDED IF IELEM=1
.005D0      *REQUIRING NODAL LOCATION INPUT.  IF IELEM=0
.01D0       *THE COMPUTER CALCULATES A LINEAR SPACING OF THE
.025D0      *NODES.
.05D0       *
.1D0        *
.15D0       *    IF THIS MANUAL ENTRY IS USED IT MUST
.2D0        *    FOLLOW INPUT OF THE VARIABLE "ITRIP"
.25D0       *    AND HAVE A VALUE FOR EACH NODAL POINT
.3D0        *
.35D0       *
.4D0        *
.45D0       *
.5D0        *
.55D0       *
.6D0        *
.65D0       *
.7D0        *
.738D0      *
.8D0        *
.85D0       *
.9D0        *
.95D0       *
1.D0 *******END OF NODAL POINT LOCATION INPUT***************
800.D0 $$$$$$$$START OF MANUAL ENTRY OF GRAPHITE TEMP FOR EACH NODE
800.D0 $
800.D0 $       $$$$$THIS INFORMATION ON TEMPERATURE AND CONCENTRATION
800.D0 $       IS ONLY REQUIRED IF IIC=0 REQUIRING MANUAL DATA INPUT
800.D0 $       FOR EACH NODAL POINT.  THE $$$$$$ DATA MUST FOLLOW DATA
800.D0 $       FOR "ITRIP" IF NODAL LOCATIONS ARE NOT BEING MANUALLY
800.D0 $       INPUT (IF IELEM=1)OR ELSE THIS DATA FOLLOWS NODAL POINT
800.D0 $       MANUAL ENTRY LOCATIONS
800.D0 $
800.D0 $       DATA MUST BE GIVEN FOR EACH NODAL POINT
800.D0 $
800.D0 $
800.D0 $
800.D0 $
800.D0 $
800.D0 $
800.D0 $
800.D0 $
800.D0 $
800.D0 $
800.D0 $
800.D0 $
800.D0 $
800.D0 $
800.D0 $$$$$$LAST MANUAL ENTRY OF GRAPHITE TEMPERATURE%%%%%%%%
800.D0 $$$$$$START MANUAL ENTRY OF AIR TEMPERATURE EACH NODE##
800.D0 $
800.D0 $
800.D0 $
800.D0 $
800.D0 $
800.D0 $
800.D0 $
800.D0 $
```

```
800.D0 $
800.D0 $
800.D0 $
800.D0 $
800.D0 $
800.D0 $
800.D0 $
800.D0 $
800.D0 $
800.D0 $
800.D0 $
800.D0 $
800.D0 $
800.D0 $
800.D0 $$$$$LAST MANUAL ENTRY OF AIR TEMPERATURE EACH NODE
.0075D0 $$$$START MANUAL ENTRY OF OXYGEN CONCENTRATION EACH NODE
.0075D0 $
.0075D0 $
.0075D0 $
.0075D0 $
.0075D0 $
.0075D0 $
.0075D0 $
.0075D0 $
.0075D0 $
.0075D0 $
.0075D0 $
.0075D0 $
.0075D0 $
.0075D0 $
.0075D0 $
.0075D0 $
.0075D0 $
.0075D0 $
.0075D0 $
.0075D0 $
.0075D0 $
.0075D0 $
.0075D0 $
.0075D0 $$$$$LAST MANUAL ENTRY OF OXYGEN CONCENTRATION EACH NODE
```

APPENDIX E: SAMPLE OUTPUT DATA FROM COMBUSTION CODE

31 NODAL POINTS

AT TIME=
0.00 S
MEDIUM THICKNESS=
.4166666666667D-01 .4166666666667D-01

NP	X	TEMP-G	DIAMETER
1	0.0000000000000000E+00	0.4000000000000000E+03	0.6944444444444444E-03
2	0.1388888888888889E-02	0.4000000000000000E+03	0.6944444444444444E-03
3	0.2777777777777778E-02	0.4000000000000000E+03	0.6944444444444444E-03
4	0.4166666666666666E-02	0.4000000000000000E+03	0.6944444444444444E-03
5	0.5555555555555555E-02	0.4000000000000000E+03	0.6944444444444444E-03
6	0.6944444444444443E-02	0.4000000000000000E+03	0.6944444444444444E-03
7	0.8333333333333331E-02	0.4000000000000000E+03	0.6944444444444444E-03
8	0.9722222222222221E-02	0.4000000000000000E+03	0.6944444444444444E-03
9	0.1111111111111111E-01	0.4000000000000000E+03	0.6944444444444444E-03
10	0.1250000000000000E-01	0.4000000000000000E+03	0.6944444444444444E-03
11	0.1388888888888889E-01	0.4000000000000000E+03	0.6944444444444444E-03
12	0.1527777777777777E-01	0.4000000000000000E+03	0.6944444444444444E-03
13	0.1666666666666666E-01	0.4000000000000000E+03	0.6944444444444444E-03
14	0.1805555555555555E-01	0.4000000000000000E+03	0.6944444444444444E-03
15	0.1944444444444444E-01	0.4000000000000000E+03	0.6944444444444444E-03
16	0.2083333333333333E-01	0.4000000000000000E+03	0.6944444444444444E-03
17	0.2222222222222222E-01	0.4000000000000000E+03	0.6944444444444444E-03
18	0.2361111111111111E-01	0.4000000000000000E+03	0.6944444444444444E-03
19	0.2499999999999999E-01	0.4000000000000000E+03	0.6944444444444444E-03
20	0.2638888888888888E-01	0.4000000000000000E+03	0.6944444444444444E-03
21	0.2777777777777777E-01	0.4000000000000000E+03	0.6944444444444444E-03
22	0.2916666666666666E-01	0.4000000000000000E+03	0.6944444444444444E-03
23	0.3055555555555555E-01	0.4000000000000000E+03	0.6944444444444444E-03
24	0.3194444444444444E-01	0.4000000000000000E+03	0.6944444444444444E-03
25	0.3333333333333333E-01	0.4000000000000000E+03	0.6944444444444444E-03
26	0.3472222222222222E-01	0.4000000000000000E+03	0.6944444444444444E-03
27	0.3611111111111110E-01	0.4000000000000000E+03	0.6944444444444444E-03
28	0.3749999999999999E-01	0.4000000000000000E+03	0.6944444444444444E-03
29	0.3888888888888888E-01	0.4000000000000000E+03	0.6944444444444444E-03
30	0.4027777777777777E-01	0.4000000000000000E+03	0.6944444444444444E-03
31	0.4166666666666666E-01	0.4000000000000000E+03	0.6944444444444444E-03

```
 AT TIME=
      8.81 S
 MEDIUM THICKNESS=
.4166666666667D-01 .4166666666667D-01
  NP          X                  TEMP-G              DIAMETER
   1 0.0000000000000000E+00 0.6171655414743030E+03 0.6944444021540727E-03
   2 0.1388888888888889E-02 0.5781984237740606E+03 0.6944444306055943E-03
   3 0.2777777777777778E-02 0.5511844753523755E+03 0.6944444380346299E-03
   4 0.4166666666666666E-02 0.5261308274882458E+03 0.6944444413489135E-03
   5 0.5555555555555555E-02 0.5035640136879362E+03 0.6944444428425697E-03
   6 0.6944444444444443E-02 0.4836232366654954E+03 0.6944444435425437E-03
   7 0.8333333333333331E-02 0.4663593795839235E+03 0.6944444438859773E-03
   8 0.9722222222222221E-02 0.4517249092494148E+03 0.6944444440630632E-03
   9 0.1111111111111111E-01 0.4395833460910138E+03 0.6944444441590080E-03
  10 0.1250000000000000E-01 0.4297262006976060E+03 0.6944444442134259E-03
  11 0.1388888888888889E-01 0.4218950356130471E+03 0.6944444442455372E-03
  12 0.1527777777777777E-01 0.4158052068913094E+03 0.6944444442651040E-03
  13 0.1666666666666666E-01 0.4111679694792949E+03 0.6944444442773239E-03
  14 0.1805555555555555E-01 0.4077084937514894E+03 0.6944444442850919E-03
  15 0.1944444444444444E-01 0.4051785413371006E+03 0.6944444442900914E-03
  16 0.2083333333333333E-01 0.4033636888937181E+03 0.6944444442933369E-03
  17 0.2222222222222222E-01 0.4020858170994085E+03 0.6944444442954588E-03
  18 0.2361111111111111E-01 0.4012020198152163E+03 0.6944444442968574E-03
  19 0.2499999999999999E-01 0.4006011841982683E+03 0.6944444442977906E-03
  20 0.2638888888888888E-01 0.4001993564763142E+03 0.6944444442984252E-03
  21 0.2777777777777777E-01 0.3999347556308410E+03 0.6944444442988702E-03
  22 0.2916666666666666E-01 0.3997630187488629E+03 0.6944444442991956E-03
  23 0.3055555555555555E-01 0.3996530135102078E+03 0.6944444442994469E-03
  24 0.3194444444444444E-01 0.3995833611737365E+03 0.6944444442996526E-03
  25 0.3333333333333333E-01 0.3995396822558629E+03 0.6944444442998301E-03
  26 0.3472222222222222E-01 0.3995124994579232E+03 0.6944444442999913E-03
  27 0.3611111111111110E-01 0.3994956957918823E+03 0.6944444443001414E-03
  28 0.3749999999999999E-01 0.3994854173856393E+03 0.6944444443002882E-03
  29 0.3888888888888888E-01 0.3994793187448693E+03 0.6944444443004240E-03
  30 0.4027777777777777E-01 0.3994760668482828E+03 0.6944444443005773E-03
  31 0.4166666666666666E-01 0.3994750372395511E+03 0.6944444443006692E-03
```

AT TIME=
17.81 S
MEDIUM THICKNESS=
.4166666666667D-01 .4166666666667D-01

NP	X	TEMP-G	DIAMETER
1	0.0000000000000000E+00	0.6944483272376198E+03	0.6944440200051797E-03
2	0.1388888888888889E-02	0.6582952483489812E+03	0.6944442750792861E-03
3	0.2777777777777778E-02	0.6330284155199859E+03	0.6944443547335164E-03
4	0.4166666666666666E-02	0.6085590421656422E+03	0.6944443969186038E-03
5	0.5555555555555555E-02	0.5853068872440880E+03	0.6944444188805062E-03
6	0.6944444444444443E-02	0.5633915122869859E+03	0.6944444303859835E-03
7	0.8333333333333331E-02	0.5429230303669187E+03	0.6944444364794849E-03
8	0.9722222222222221E-02	0.5239878470762538E+03	0.6944444397590113E-03
9	0.1111111111111111E-01	0.5066449982116862E+03	0.6944444415612797E-03
10	0.1250000000000000E-01	0.4909237200244683E+03	0.6944444425767153E-03
11	0.1388888888888889E-01	0.4768226385980613E+03	0.6944444431650298E-03
12	0.1527777777777777E-01	0.4643106220267744E+03	0.6944444435161306E-03
13	0.1666666666666666E-01	0.4533292103391948E+03	0.6944444437320398E-03
14	0.1805555555555555E-01	0.4437963847202381E+03	0.6944444438687254E-03
15	0.1944444444444444E-01	0.4356113128753018E+03	0.6944444439576309E-03
16	0.2083333333333333E-01	0.4286596365129955E+03	0.6944444440168827E-03
17	0.2222222222222222E-01	0.4228188585575783E+03	0.6944444440572177E-03
18	0.2361111111111111E-01	0.4179634359788205E+03	0.6944444440851723E-03
19	0.2499999999999999E-01	0.4139692729896838E+03	0.6944444441048360E-03
20	0.2638888888888888E-01	0.4107174182763530E+03	0.6944444441188342E-03
21	0.2777777777777777E-01	0.4080968793508916E+03	0.6944444441288955E-03
22	0.2916666666666666E-01	0.4060065623126001E+03	0.6944444441361831E-03
23	0.3055555555555555E-01	0.4043564178987307E+03	0.6944444441414949E-03
24	0.3194444444444444E-01	0.4030679223461711E+03	0.6944444441453872E-03
25	0.3333333333333333E-01	0.4020740463757375E+03	0.6944444441482521E-03
26	0.3472222222222222E-01	0.4013188723800529E+03	0.6944444441503701E-03
27	0.3611111111111110E-01	0.4007570137582123E+03	0.6944444441519371E-03
28	0.3749999999999999E-01	0.4003529789248906E+03	0.6944444441530992E-03
29	0.3888888888888888E-01	0.4000805996527675E+03	0.6944444441539341E-03
30	0.4027777777777777E-01	0.3999226594325125E+03	0.6944444441545535E-03
31	0.4166666666666666E-01	0.3998706998552636E+03	0.6944444441548335E-03

```
 AT TIME=
     26.56 S
MEDIUM THICKNESS=
.4166666666667D-01 .4166666666667D-01
 NP          X                  TEMP-G              DIAMETER
  1 0.0000000000000000E+00 0.6306595038438272E+03 0.6944429267898032E-03
  2 0.1388888888888889E-02 0.6399241320641830E+03 0.6944437360540249E-03
  3 0.2777777777777778E-02 0.6447192511167083E+03 0.6944440181040645E-03
  4 0.4166666666666666E-02 0.6406985836760575E+03 0.6944441916810881E-03
  5 0.5555555555555555E-02 0.6302556153620338E+03 0.6944442957791966E-03
  6 0.6944444444444443E-02 0.6156188718308147E+03 0.6944443573613218E-03
  7 0.8333333333333331E-02 0.5986698701861527E+03 0.6944443933015021E-03
  8 0.9722222222222221E-02 0.5807979040862021E+03 0.6944444141127005E-03
  9 0.1111111111111111E-01 0.5629290453016817E+03 0.6944444261547878E-03
 10 0.1250000000000000E-01 0.5456325613672719E+03 0.6944444331631678E-03
 11 0.1388888888888889E-01 0.5292359938247957E+03 0.6944444372871645E-03
 12 0.1527777777777777E-01 0.5139161110240054E+03 0.6944444397507130E-03
 13 0.1666666666666666E-01 0.4997594668844450E+03 0.6944444412492834E-03
 14 0.1805555555555555E-01 0.4867985002414993E+03 0.6944444421795931E-03
 15 0.1944444444444444E-01 0.4750316490868472E+03 0.6944444427698287E-03
 16 0.2083333333333333E-01 0.4644343493352758E+03 0.6944444431527831E-03
 17 0.2222222222222222E-01 0.4549653630104841E+03 0.6944444434068504E-03
 18 0.2361111111111111E-01 0.4465709326513697E+03 0.6944444435790780E-03
 19 0.2499999999999999E-01 0.4391880102692778E+03 0.6944444436982122E-03
 20 0.2638888888888888E-01 0.4327471084903999E+03 0.6944444437821565E-03
 21 0.2777777777777777E-01 0.4271749671005763E+03 0.6944444438422836E-03
 22 0.2916666666666666E-01 0.4223970689333552E+03 0.6944444438859626E-03
 23 0.3055555555555555E-01 0.4183399816653412E+03 0.6944444439180605E-03
 24 0.3194444444444444E-01 0.4149334943623446E+03 0.6944444439418518E-03
 25 0.3333333333333333E-01 0.4121125315457292E+03 0.6944444439595736E-03
 26 0.3472222222222222E-01 0.4098188488450426E+03 0.6944444439727761E-03
 27 0.3611111111111110E-01 0.4080025338059548E+03 0.6944444439825334E-03
 28 0.3749999999999999E-01 0.4066233572360078E+03 0.6944444439895999E-03
 29 0.3888888888888888E-01 0.4056520065572266E+03 0.6944444439944511E-03
 30 0.4027777777777777E-01 0.4050713541567405E+03 0.6944444439974719E-03
 31 0.4166666666666666E-01 0.4048773671370597E+03 0.6944444439985787E-03
```

LIST OF REFERENCES

1. Fontenot, J., "Graphite-Epoxy Composite Material Response to Carrier Deck Fires", Naval Weapons Center, NWC Technical Memorandum 3351, November, 1979

2. Vatikiotis, C., "Analysis of Combustion and Heat Transfer in a Porus Graphite Medium", M.S. Thesis, Naval Postgraduate School, Monterey, CA, June, 1980.

3. Vatikiotis, C., "A Combustion Heat Transfer Model for a Porous Media", Doctoral Thesis, Naval Postgraduate School, Monterey, CA, June, 1982.

4. Thomson, W.T., Theory of Vibration with Applications, Third Edition, p. 37, Prentice Hall Publishing Co., 1972.

5. Logan, D.L., Mechanics of Materials, p. 563, Harper Collins Publishers Inc., 1991.

6. Rosen, B.W., "Mechanics of Composite Strengthening", Fiber Composite Materials, papers presented at a seminar of the American Society for Metals,p. 74, October 17 and 18, 1964.

7. Akin, J.E., Finite Element Analysis for Undergraduates, p. 37, Academic Press, 1986.

8. Akin, J.E., Application and Implementation of Finite Element Methods, Academic Press, 1982.

INITIAL DISTRIBUTION LIST

1.	Defense Technical Information Center Cameron Station Alexandria, VA 22304-6145	2
2.	Library, Code 52 Naval Postgraduate School Monterey, CA 93940-5002	2
3.	Chairman, Code ME Department of Mechanical Engineering Naval Postgraduate School Monterey, CA 93940-5000	1
4.	Professor David Salinas, Code ME/SA Department of Mechanical Engineering Naval Postgraduate School Monterey, CA 93943-5000	3
5.	Mr. Edward Faxlanger Sr. 5292 W. Mt. Morris Rd. Mt. Morris, MI 48458	3
6.	Naval Engineering Curricular Office, Code 34 Naval Postgraduate School Monterey, CA 93943-5000	1
7.	Professor Young Kwon, Code ME/KW Department of Mechanical Engineering Naval Postgraduate School Monterey, CA 93943-5000	3